

**SYNTHESIS AND CHARACTERIZATION OF
HOLE-TRANSPORTING MATERIALS BASED ON
8-HYDROXYQUINOLINE DERIVATIVES FOR
ORGANIC LIGHT-EMITTING DIODES**



**A Thesis Submitted in Partial Fulfillment of the Requirements for the
Degree of Master of Science in Chemistry
Suranaree University of Technology
Academic Year 2015**

การสังเคราะห์และพิสูจน์เอกลักษณ์สารส่งผ่านประจุบวกที่เป็นอนุพันธ์ของ
8-ไฮดรอกซีควิโนลิน สำหรับใช้ในไดโอดเปล่งแสงอินทรีย์



วิทยานิพนธ์นี้เป็นส่วนหนึ่งของการศึกษาตามหลักสูตรปริญญาวิทยาศาสตรมหาบัณฑิต
สาขาวิชาเคมี
มหาวิทยาลัยเทคโนโลยีสุรนารี
ปีการศึกษา 2558

**SYNTHESIS AND CHARACTERIZATION OF HOLE-
TRANSPORTING MATERIALS BASED ON
8-HYDROXYQUINOLINE DERIVATIVES FOR ORGANIC
LIGHT-EMITTING DIODES**

Suranaree University of Technology has approved this thesis submitted in partial fulfillment of the requirements for a Master's Degree.

Thesis Examining Committee

(Assoc. Prof. Dr. Jatuporn Wittayakun)

Chairperson

(Assoc. Prof. Dr. Visit Vao-soongnern)

Member (Thesis Advisor)

(Prof. Dr. Vinich Promarak)

Member

(Asst. Prof. Dr. Thanaporn Manyum)

Member

(Prof. Dr. Sukit Limpijumnong)

Vice Rector for Academic Affairs
and Innovation

(Prof. Dr. Santi Maensiri)

Dean of Institute of Science

ปัญญา เอิบอ้อม : การสังเคราะห์และพิสูจน์เอกลักษณ์สารส่งผ่านประจุบวกที่เป็นอนุพันธ์ของ 8-ไฮดรอกซีควิโนลีน สำหรับใช้ในไดโอดเปล่งแสงอินทรีย์ (SYNTHESIS AND CHARACTERIZATION OF HOLE-TRANSPORTING MATERIALS BASED ON 8-HYDROXYQUINOLINE DERIVATIVES FOR ORGANIC LIGHT-EMITTING DIODES) อาจารย์ที่ปรึกษา : รองศาสตราจารย์ ดร.วิสิทธิ์ แวสูงเนิน, 77 หน้า.

สารส่งผ่านประจุบวกตัวใหม่ที่เป็นอนุพันธ์ของ 8-ไฮดรอกซีควิโนลีน ซึ่งคือ **HQG1** และ **HQG2** ได้ถูกออกแบบและสังเคราะห์สำหรับใช้ในไดโอดเปล่งแสงอินทรีย์ ในการสังเคราะห์ต้องมีการแต่ละขั้นตอนซึ่งประกอบไปด้วย 5-bromo-8-tosylquinoline (**2**), 5-(4-hydroxymethyl)phenyl)-8-tosylquinoline (**3**) และ 5-(4-chloromethyl)phenyl)-8-tosylquinoline (**4**) ซึ่งถูกสังเคราะห์ด้วยปฏิกิริยา tosylation, Suzuki cross coupling และ halogenation ตามลำดับ โมเลกุลเป้าหมายคือ **HQG1** และ **HQG2** ได้ถูกสังเคราะห์ด้วยปฏิกิริยา Gn-substitution และ detosylation จากสาร 5-(4-chloromethyl)phenyl)-8-tosylquinoline (**4**) และ 5-(4-(Gn)methyl)phenyl)-8-tosylquinoline **HQOTsGn** โมเลกุล **HQG1** และ **HQG2** ถูกระบุเอกลักษณ์ด้วยเทคนิค $^1\text{H-NMR}$, $^{13}\text{C-NMR}$ และถูกศึกษาคุณสมบัติด้วยเทคนิค UV-Visible spectroscopy, fluorescence spectroscopy, differential scanning calorimetry (DSC) และ thermogravimetric analysis (TGA) สุดท้ายนี้โมเลกุลเป้าหมาย **HQG1** และ **HQG2** ถูกคาดหวังที่จะเป็นวัสดุส่งผ่านประจุบวกที่มีลักษณะเป็นอสัญฐานและมีความเสถียรทางความร้อนที่อุณหภูมิสูงสำหรับใช้ในไดโอดเปล่งแสงอินทรีย์

สาขาวิชาเคมี

ปีการศึกษา 2558

ลายมือชื่อนักศึกษา_____

ลายมือชื่ออาจารย์ที่ปรึกษา_____

ลายมือชื่ออาจารย์ที่ปรึกษาร่วม_____

PANYA UERB-IM : SYNTHESIS AND CHARACTERIZATION OF HOLE-
TRANSPORTING MATERIALS BASED ON 8-HYDROXYQUINOLINE
DERIVATIVES FOR ORGANIC LIGHT-EMITTING DIODES. THESIS
ADVISOR : ASSOC. PROF. VISIT VAO-SOONGNERN, Ph.D. 77 PP.

HOLE-TRANSPORTING MATERIALS/ ORGANIC LIGHT-EMITTING DIODES

New hole-transporting materials based on 8-hydroxyquinoline derivative (**HQG1-HQG2**) have been designed and synthesized for use in high performance OLEDs. The key intermediates 5-bromo-8-tosylquinoline (**2**), 5-(4-(hydroxymethyl)phenyl)-8-tosyl-quinoline (**3**) and 5-(4-(chloromethyl)phenyl)-8-tosyl-quinoline (**4**) were obtained by tosylation, Suzuki cross coupling and halogenation, respectively. Target molecules **HQG1** and **HQG2** were synthesized by Gn-substitution and detosylation from 5-(4-(chloromethyl)-phenyl)-8- tosylquinoline (**4**) and 5-(4-((Gn)methyl)phenyl)-8-tosylquinoline **HQOTsGn**. These **HQG1** and **HQG2** were characterized by $^1\text{H-NMR}$ and $^{13}\text{C-NMR}$, UV-Visible spectroscopy, fluorescence spectroscopy, differential scanning calorimetry (DSC), and thermogravimetric analysis (TGA). Finally, the target molecules **HQG1** and **HQG2** were expected to be used as high efficient amorphous hole-transporting material with high thermal stability for OLEDs.

School of Chemistry

Academic Year 2015

Student's Signature_____

Advisor's Signature_____

Co-advisor's Signature_____

ACKNOWLEDGEMENTS

The research work presented in this thesis carried out at Center for Organic Electronic and Alternative Energy (COEAE) during the period January 2013 – December 2015.

I would like to thank Prof. Dr. Vinich Promarak, our electronic group leader and my supervisor, for allowing me to undertake this project, all the brilliant ideas, his enthusiasm, advice and guiding me throughout the years, help and for bringing me to the “world of organic synthesis” connected to the “world of electro-optical devices”. His advice was most valuable to understand the obtained results and to determine the next steps for the research presented in this thesis.

I also would like to thank to my thesis advisor, Assoc. Prof. Dr. Visit Vao-soongnern for there constructions comments and suggestion. In addition, I am grateful for the teachers of School of Chemistry, thesis examining committee, including Assoc. Prof. Dr. Jatuporn Wittayakun and Asst. Prof. Dr. Thanaporn Manyum for suggestions and all their help.

I would like to thank everyone in the electronic group for contributed and helped me to make this research work possible at Suranaree University of Technology.

Finally, I want to acknowledge the School of Chemistry at Suranaree University of Technology and SUT for scholarship.

Panya Uerb-im

CONTENTS

	Page
ABSTRACT IN THAI.....	I
ABSTRACT IN ENGLISH	II
ACKNOWLEDGEMENTS	III
CONTENTS.....	IV
LIST OF TABLES	VIII
LIST OF FIGURES	IX
CHAPTER	
I INTRODUCTION.....	1
1.1 Organic light-emitting diodes (OLEDs).....	1
1.1.1 Evolution of OLEDs	1
1.1.2 OLEDs: structure and operation	2
1.1.3 Working principle of OLEDs	5
1.2 Materials used for different layers of OLEDs.....	6
1.2.1 Substrate materials	6
1.2.2 Anode materials	6
1.2.3 Hole injection layer (HIL).....	7
1.2.4 Hole transport layer (HTL).....	7
1.2.5 Emissive layer (EML).....	8

CONTENTS (Continued)

	Page
1.2.6 Electron transport layer (ETL).....	9
1.2.7 Electron injection layer (EIL).....	10
1.2.8 Cathode materials.....	10
II LITERATURE REVIEW	11
2.1 OLEDs.....	11
2.1.1 TDCTA.....	12
2.1.2 C1Q2-T.....	12
2.1.3 PCTrz	13
2.1.4 36FCzG2	14
2.1.5 Cz-CBP.....	15
2.1.6 CPMP.....	15
2.1.7 TPA-Cz.....	16
2.1.8 G2F3.....	17
III EXPERIMENTAL	20
3.1 Chemical and reagents.....	20
3.2 Characterization techniques	20
3.2.1 Nuclear magnetic resonance (NMR).....	21
3.2.2 Fourier Transform Infrared Spectroscopy (FT-IR).....	21
3.2.3 UV-Visible spectroscopy	21

CONTENTS (Continued)

	Page
3.2.4 Differential scanning calorimetry (DSC) and thermo gravimetric analysis (TGA)	21
3.2.5 Mass spectroscopy	21
3.2.6 Melting point (m.p.)	21
3.2.7 Fluorescence spectroscopy	22
3.3 Experimental	22
3.3.1 5-Bromo-8-tosylquinoline (2).....	22
3.3.2 5-(4-(Hydroxymethyl)phenyl)-8-tosylquinoline (3)	23
3.3.3 5-(4-(Chloromethyl)phenyl)-8-tosylquinoline (4)	23
3.3.4 5-(4-((G1)methyl)phenyl)-8-tosylquinoline (HQOTsG1).....	24
3.3.5 5-(4-((G1)methyl)phenyl)-8-hydroxyquinoline (HQG1).....	25
3.3.6 5-(4-((G2)methyl)phenyl)-8-tosylquinoline (HQOTsG2).....	25
3.3.7 5-(4-((G2)methyl)phenyl)-8-hydroxyquinoline (HQG2).....	26
IV RESULTS AND DISCUSSION	28
4.1 Synthesis	28
4.1.1 5-Bromo-8-tosylquinoline (2).....	30
4.1.2 5-(4-(Hydroxymethyl)phenyl)-8-tosylquinoline (3)	31
4.1.3 5-(4-(Chloromethyl)phenyl)-8-tosylquinoline (4)	33
4.1.4 5-(4-((G1)methyl)phenyl)-8-tosylquinoline (HQOTsG1).....	34

CONTENTS (Continued)

	Page
4.1.5 5-(4-((G1)methyl)phenyl)-8-hydroxyquinoline (HQG1).....	36
4.1.6 5-(4-((G2)methyl)phenyl)-8-tosylquinoline (HQOTsG2).....	38
4.1.7 5-(4-((G2)methyl)phenyl)-8-hydroxyquinoline (HQG2).....	39
4.2 Optical properties	41
4.3 Thermal properties	44
V CONCLUSION	46
REFERENCES.....	47
APPENDICES.....	55
APPENDIX A CALCULATION: % YIELD.....	56
APPENDIX B THESIS OUTPUT	76
CURRICULUM VITAE.....	77

LIST OF TABLES

Table	Page
1.1 Summary of the physical data of HQGn (n = 1-2)	44
1.2 Thermal properties of HQGn (n = 1-2).....	45



LIST OF FIGURES

Figure		Page
1.1	The structure of the first single layer OLEDs	3
1.2	First double-layer OLEDs configuration	4
1.3	General structure of multilayer OLEDs devices	5
1.4	Working principle of OLEDs	6
1.5	The structure of m-MTDATA and CuPc	7
1.6	The structure of TPD, NPD, CBP, and CDBP	8
1.7	The structure of materials in the emissive layer	9
1.8	The structure of Alq ₃ and ADN	9
2.1	The structure of NPD and TPD	11
2.2	The structure of TDCTA	12
2.3	The structure of C1Q2-T	13
2.4	The structure of PCTrz	14
2.5	The structure of 36FCzG2	14
2.6	The structure of Cz-CBP	15
2.7	The structure of CPMP	16
2.8	The structure of TPA-Cz	17
2.9	The structure of G2F3	18
2.10	The structure of G1-G2 carbazole	18

LIST OF FIGURES (Continued)

Figure	Page
2.11 The structure of HQG1 and HQG2.....	19
4.1 Synthesis of hole-transporting materials HQG1 and HQG2 for OLEDs.....	29
4.2 The synthesis of compound 2.....	30
4.3 ¹ H-NMR of compound 2 in CDCl ₃	31
4.4 The synthesis of compound 3.....	32
4.5 Generally accepted mechanism for Suzuki reaction in a homogeneous phase.....	32
4.6 ¹ H-NMR of compound 3 in CDCl ₃	33
4.7 The synthesis of compound 4.....	34
4.8 ¹ H-NMR of compound 4 in CDCl ₃	34
4.9 The synthesis of HQOTsG1.....	35
4.10 ¹ H-NMR of HQOTsG1 in CDCl ₃	36
4.11 The synthesis of HQG1.....	37
4.12 ¹ H-NMR of HQG1 in CDCl ₃	37
4.13 The synthesis of HQOTsG2.....	38
4.14 ¹ H-NMR of HQOTsG2 in CDCl ₃	39
4.15 The synthesis of HQG2.....	40
4.16 ¹ H-NMR of HQG2 in CDCl ₃	40
4.17 Absorption spectra of HQG1 and HQG2 in CH ₂ Cl ₂	42
4.18 Fluorescence spectra of HQG1 and HQG2 in CH ₂ Cl ₂	43
4.19 The energy level of HQG1 and HQG2.....	43

LIST OF FIGURES (Continued)

Figure	Page
4.20 DSC traces of HQG1 and HQG2 measured under nitrogen atmosphere at heating rate of 10 °C/min	44
4.21 TGA of HQG1 and HQG2 measured under nitrogen atmosphere at heating rate of 10 °C/min	45



CHAPTER I

INTRODUCTION

Understanding the chemical and photophysical properties of electroluminescent (EL) materials is assistant in receiving an in-depth grasp of organic light-emitting mechanisms. In organic light-emitting diodes (OLEDs), there are three major physical processes exist: (i) charge injection and transport, (ii) charge recombination and excitons energy transfer, and (iii) light emission (Gutmann et al., 1981). All of these processes shown important role in such factors as the external quantum efficiency, turn-on voltage and luminance of OLEDs (Dresner et al., 1969). Organic light-emitting material properties such as mobility, energy level and thermal properties have a important effect on the aforementioned three processes (Tang and Vanslyke, 1987).

1.1 Organic light-emitting diodes (OLEDs)

1.1.1 Evolution of OLEDs

OLEDs was improved from cathode ray tube (CRT), liquid crystal displays (LCDs), and light-emitting diodes (LEDs). The cathode ray tube (CRT) has the brightness of saturated colors and spread in many the world (Rajagopal et al., 1998). Nevertheless, the CRT is intrinsically heavy, bulky, inefficient and expensive. Liquid crystal displays (LCDs) are narrow viewing angles when compared to the CRT. However, the production of large area LCDs has been prohibitively expensive and difficult (Wohlgenannt et al., 2001). Light-emitting diodes (LEDs) furnish several

advantages over the CRT and LCDs technologies. LEDs should have lower energy consumption, but the methods required for produce the devices are difficult and costly, especially for large area displays (Tandon et al., 2003).

OLEDs are interested as powerful candidates because they are area lighting sources, which can be driven at low voltages as just several volts. This can be achieved by using the number of light emissive materials such as blue, green, and red. OLEDs generate light in much the similar way that common LEDs do, other than that the positive and negative charges create in organic compounds more than in crystalline semiconductors (Seung et al., 2002). They emit light across the visible, ultraviolet and infrared wavelengths, with very high brightness and have the potential for energy efficient solutions (Chen et al., 2003). Moreover, OLEDs technology presents several advantages on conventional lighting, it is slimness and thickness of the OLED panel for lighting applications (Huang et al., 2006) such a characteristic of OLED lighting to be placed instantly on coverings more than using fixtures (Ide et al., 2008).

1.1.2 OLEDs: structure and operation

A single-layer OLED compose of an organic layer sandwiched between two electrodes. This organic layer has three main functions which are hole transport, electron transport and light emission (Kallmann and Pope, 1960). In this respect, the injection of both the charges should be same else the device which has low efficiency owing to the excess of electrons and holes are cannot combine (Agrawal and Jenekhe, 1996).

In 1960, Pope et al. observed the electroluminescence of anthracene using silver electrode at 400 V. The structure of this device is shown in **Figure 1.1**

Nevertheless, researchers were not interested in that time because it used high voltage and had poor device performance (Pope et al., 1963).

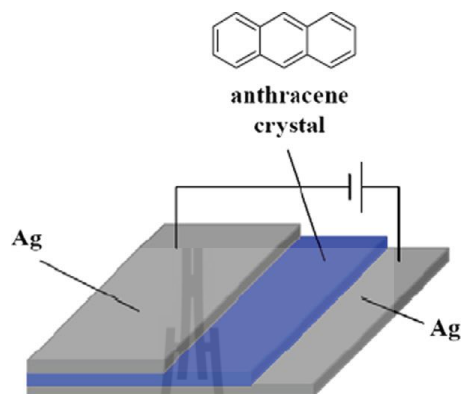


Figure 1.1 The structure of the first single layer OLEDs (Pope et al., 1963).

The first double layer diode device was reported at Eastman Kodak by Ching W. Tang and Steven Vanslyke in 1987. This device used a novel two-layer structure with separate hole transporting and electron transporting layers which affect to the result of recombination and light emission appears in the middle of the organic layer. This resulted in the decrease of work voltage and increase efficiency which led to the era of OLED research and device production. Luminance exceeds 1000 cd/m^2 below 10 V with a quantum efficiency of 1% photon/electron was succeeded. **Figure 1.2** shows the first double-layer organic light emitting diode and the structure of the Alq_3 and Diamine organic materials (Tang and Vanslyke, 1987).

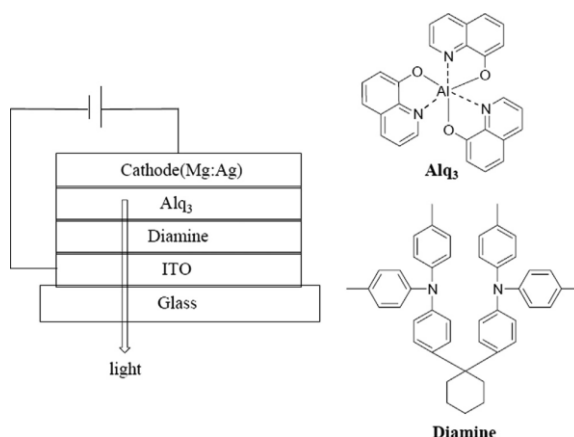


Figure 1.2 First double-layer OLEDs configuration (Tang et al., 1963).

In multi-layer OLED, they compose of cathode layer namely ITO glass plate, hole injection layer (HIL), hole transport layer (HTL), emitting layer (EML), electron transport layer (ETL) and anode. The materials to be used in order to divergent layers for OLEDs should appropriate the requirements like high luminescence efficiency, narrow spectra and correct CIE coordinates, adequate conductivity, good temperature stability, good oxidative stability (water, oxygen) and good radical cation/anion stability, also they should not degrade during sublimation (Sano et al., 1995).

In 1995, Sano et al. produced multi-layer EL cell with the emission of an Eu-complex formed by vacuum-vapor deposition technique. They used 1AZM-HEX (host material) emitting layer and Eu(TTA)₃Phen (dopant) in **Figure 1.3**.

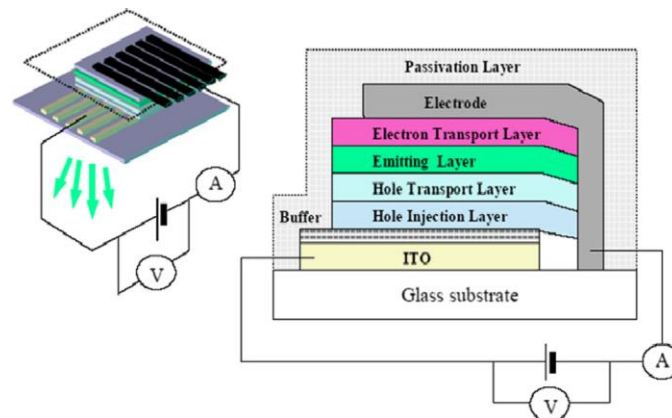


Figure 1.3 General structure of multilayer OLEDs devices (Sano et al., 1995).

1.1.3 Working principle of OLEDs

When the electric field is applied between the anode and the cathode. The electrons and holes are injected from the cathode and the anode into the organic layers. The electron injection layer and the hole injection layer should be matched between the cathode and the anode, electrons and holes are injected into the electron transport layer and hole transport layer (Thejokalyani and Dhoble, 2012).

After that, the electrons and holes emigrate into electron transport layer (ETL) and hole transport layer (HTL). When electrons and holes are excited, they move by means of charge-hopping mechanism, straight the electron and hole transport materials (ETMs and HTMs) and ultimately into the emissive layer (EML) (Thejokalyani and Dhoble, 2012).

Finally, the charges can converge at the emissive layer. Immediately, the contrary recombine to form an exciton, they give rise to light emission and the color of the light depends on the type of organic molecule in the emissive layer (Thejokalyani and Dhoble, 2012). Light emitting mechanism from an OLED device is shown in **Figure 4**.

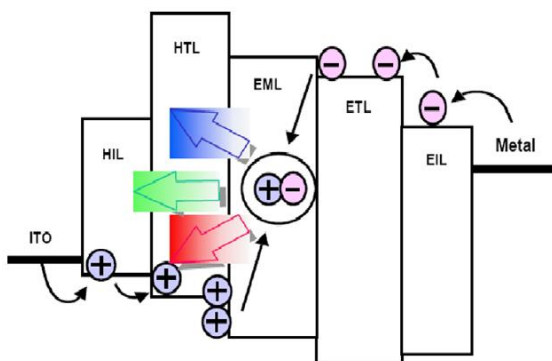


Figure 1.4 Working principle of OLEDs (Thejokalyani et al., 2012).

1.2 Materials used for different layers of OLEDs

1.2.1 Substrate materials

Substrate is a necessary ingredient of the device or display. The substrate conditions comprise high transparency, low roughness, high surface finish, high flatness, proportionally stable at processing temperatures and possess high resistance against HNO_3 , HF , NaOH . In general glass is used for substrate because it is strict and occupies high glass-transition-temperature. In addition, plastic sheets such as clear plastic, metal foil, which is transparent and can likewise be used as substrate (Wyckhoff , 1963).

1.2.2 Anode materials

Materials that used as an anode in OLEDs should be high transparent for inject holes into organic layers and highly conductive in order to succeed a device with high performance and efficiency. Indium tin oxide (ITO) is extensively used as anode material (Han et al., 2012).

1.2.3 Hole injection layer (HIL)

This layer injects holes from anode to the emissive layer. The materials should be high mobility, electron blocking capacity and high glass transition temperature, and the examples of material are 4,4',4'-tris(3-methylphenylphenylamino) triphenylamine (m-MTDATA) and copper phthalocyanine (CuPc) (Han et al., 2012).

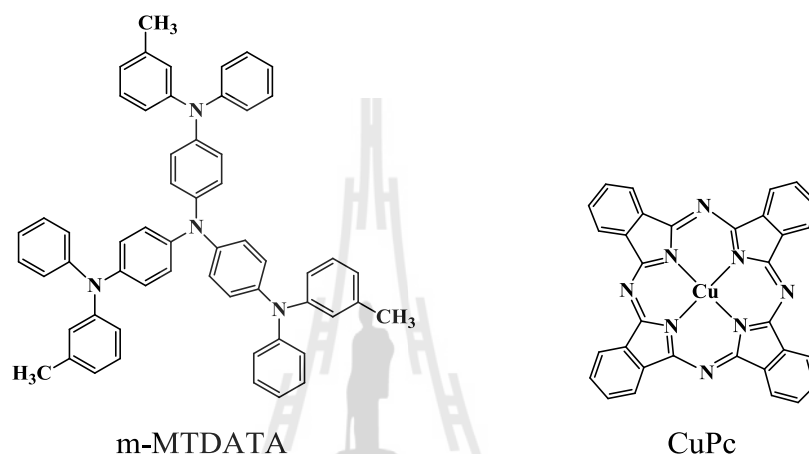


Figure 1.5 The structure of m-MTDATA and CuPc (Tae-Hee et al., 2012).

1.2.4 Hole transport layer (HTL)

Materials that used as HTL in OLEDs should be low ionization potential, low electron affinities and high hole mobility normally function as hole transporting materials by accepting and transporting hole carriers with a positive charge. The most common hole transport materials are 1,1'-biphenyl-4,4'-diamine (TPD), N'-bis(1-naphthylphenyl)-1,1'-biphenyl-4,4'-diamine (NPB), 1,10-bis(di-4-tolylaminophenyl) cyclohexane (TAPC), CBP, and CDBP (Han et al., 2012).

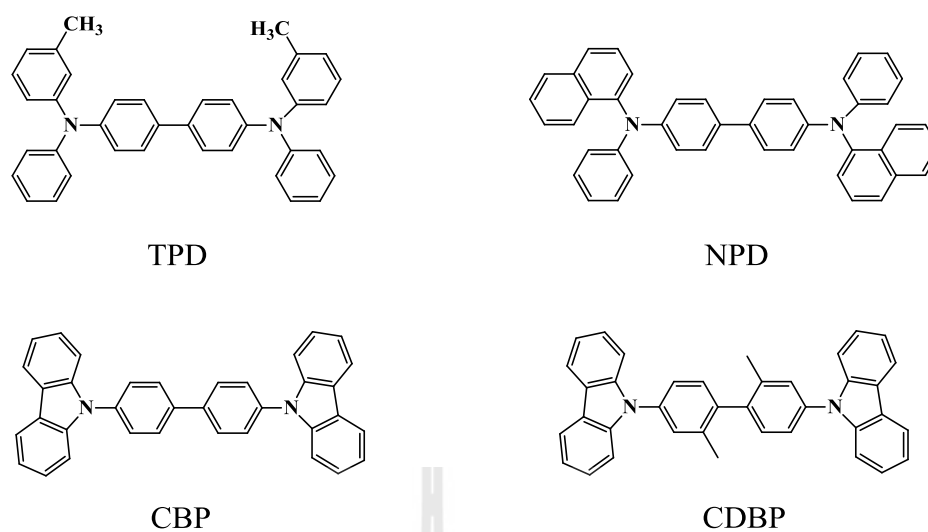


Figure 1.6 The structure of TPD, NPD, TPAC and carbazole (Tae-Hee et al., 2012).

1.2.5 Emissive layer (EML)

The emissive layer (EML) is located between HTL and ETL and emitted in visible region, normally understood as emissive layer (EML). These materials can be made from organic molecules or polymers or dendrimers with high efficiency, lifetime and colour purity. The EML materials should have a high glass-transition temperature. The examples of materials in EML are organic molecule, polymer, and dendrimer (Han et al., 2012).

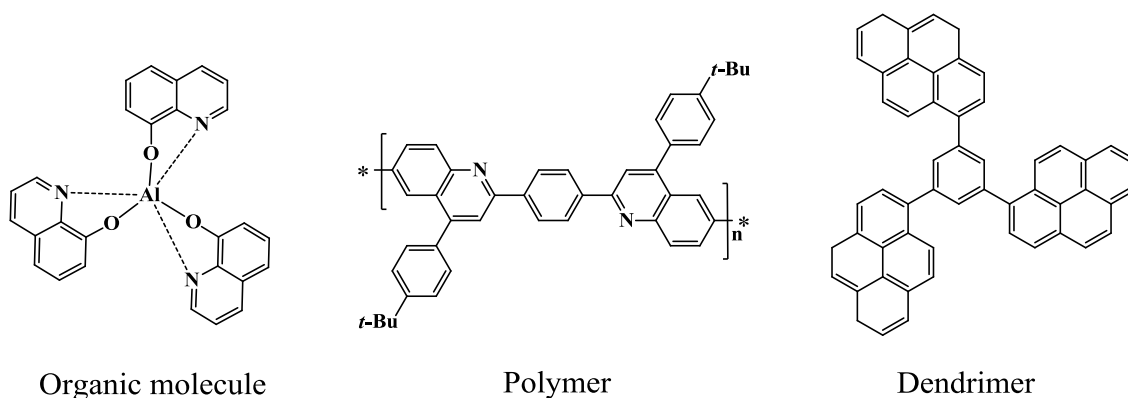


Figure 1.7 The structure of materials in the emissive layer (Tae-Hee et al., 2012).

1.2.6 Electron transport layer (ETL)

The materials of ETL should be electron transporting and hole blocking properties, high electron affinities together with high ionization. The electron transporting materials function for accept negative charges and allow them to move through the molecules. The examples of materials in ETL are aluminium tris-8-hydroxyquinoline (Alq_3) and 9,10-di-(2-naphthyl)-anthracene (ADN) (Han et al., 2012).

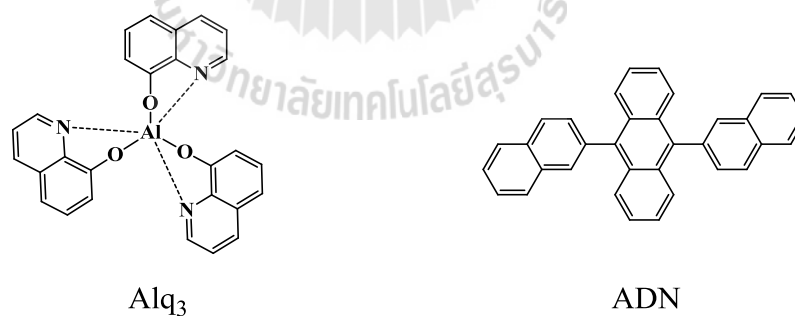


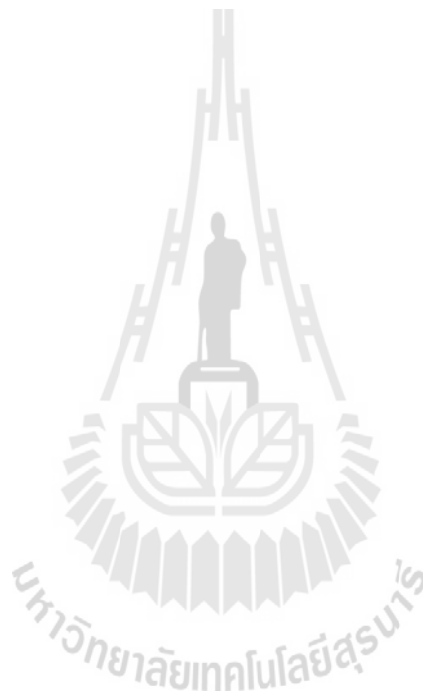
Figure 1.8 The structure of Alq_3 and ADN (Tae-Hee et al., 2012).

1.2.7 Electron injection layer (EIL)

The electron injection layer (EIL) inject electron from cathode into emitting layers. The example of material are MgO , CsF , and NaCl (Han et al., 2012).

1.2.8 Cathode materials

The function of cathode inject electrons into emitting layers. The examples of material are lithium, calcium, and magnesium (Han et al., 2012).



CHAPTER II

LITERATURE REVIEW

2.1 OLEDs

Organic light-emitting diodes (OLEDs) based on organic small molecules have been a growing interest because of their potential use in flat panel displays and lighting (Griniene et al., 2011). Recently, many researchers have improved efficiency of hole-transporting layers (HTLs) for hole injection from the anode into the emitting layer in multilayer devices. The most commonly used hole transporting materials (HTMs), N,N'-diphenyl-N,N'-bis(1-naphthyl)-(1,1'-biphenyl)-4,4'-diamine (**NPB**) and N,N'-bis(3-methylphenyl)-N,N'-bis(phenyl)benzidine (**TPD**), have provide high charge carrier mobility. However, they have low glass transition temperature (T_g) (60 °C for TPD and 98 °C for NPB) (Singh et al., 2015). Therefore, it is of interest to use carbazole as hole-transporting material (HTM) owing to its high glass transition temperature.

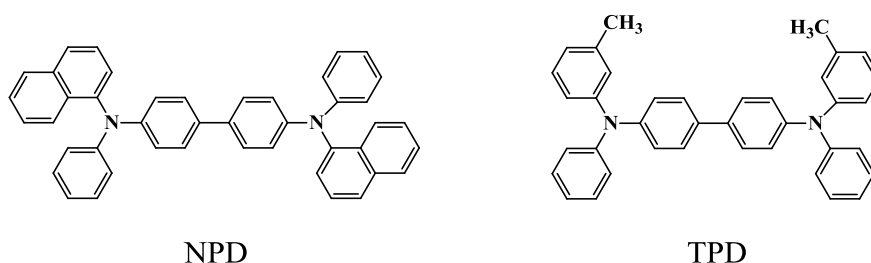


Figure 2.1 The structure of NPD and TPD (Tae-Hee et al., 2012).

Many carbazole derivatives have been widely studied for using in hole-transport materials (HTMs) because their good hole-transport and luminescent (Wang et al., 2008). It was also investigated that thermal stability of organic compounds and was exceedingly improved on appearance of a carbazole moiety in the structure.

2.1.1 TDCTA

Chen and co-workers (2003) synthesized **TDCTA** from an amination reaction between three equivalents of 13H-dibenzo[*a,g*]carbazole and one equivalent of tris(4-bromophenyl)amine. The emission wavelength of **TDCTA** shown at 397 nm. In addition, **TDCTA** has the thermal decomposition temperature (T_d) was 575 °C and the glass transition temperature (T_g) was 212 °C.

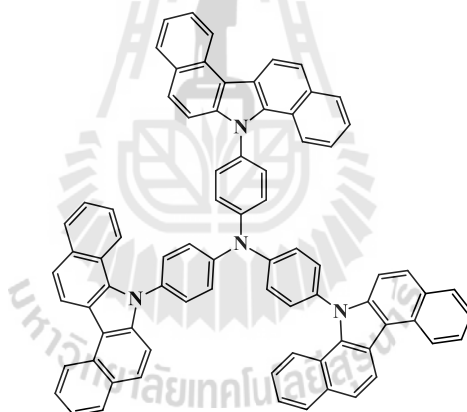


Figure 2.2 The structure of **TDCTA** (Chen et al., 2003).

2.1.2 C1Q2-T

Ananth reddy and co-workers (2011) designed **C1Q2-T** which is bipolar, carbazole/ quinoxaline coupled hybrids having hole transporting (carbazole) and electron transporting (quinoxaline) properties. The unique shape/geometry of these carbazole/quinoxaline hybrids further offers better thermal and film forming properties. **C1Q2-T** has glass transition temperature (T_g) of 132 °C and λ_{em} at 437

nm. The fluorescence quantum yields (Φ_f) was 0.35 in dilute toluene solution using 9,10-diphenylanthracene ($\Phi_f = 0.9$) as a standard.

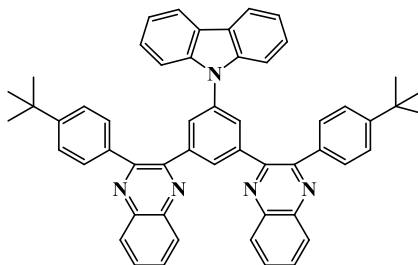


Figure 2.3 The structure of **C1Q2-T** (Ananth reddy et al., 2011).

2.1.3 PCTrz

Rothmann and co-workers (2011) present 2-(4-(3,6-dimethylcarbazol-9-yl)-phenoxy)-bis-4,6-biscarbazolyl-1,3,5-triazine **PCTrz** as a new bipolar host material for blue phosphorescent OLEDs. **PCTrz** comprises one hole conducting phenoxy-carbazole and one electron deficient biscarbazolyltriazine moiety, which are connected by an ether bond. **PCTrz** has glass transition temperature (T_g) = 148 °C and λ_{em} at 473 nm. The Phosphorescent organic light emitting diodes was fabricated using 10 nm thick layer of **DPBIC** followed as exciton and electron blocker. The 20 nm thick emission layer consisted of **PCTrz** doped with 16% Flrpic. The hole-blocking and electron-conduction layers consisted of 5 nm **DBFSi** and 40 nm BCP. The devices were finalized by deposition of a LiF (0.7 nm)/Al (100 nm) cathode. Maximum current efficiency of 13.5 cd/A was observed.

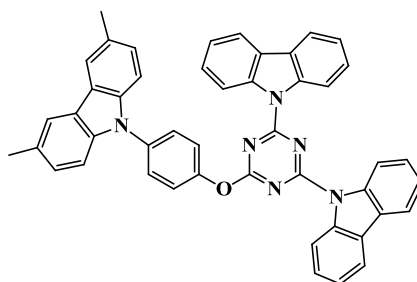


Figure 2.4 The structure of PCTrz (Rothmann et al., 2011).

2.1.4 36FCzG2

Qian and co-workers (2013) designed and synthesized the 9,9'-(9-phenyl-9-(9-phenyl-9H-carbazol-3-yl)-9H-fluorene-3,6-diylbis(3,6-bis(3,6-di-tert-butyl-9H-fluoren-9-yl)-9H-carbazole) (**36FCzG2**), using a 3,6-substituted fluorene derivatives as the rigid core with two carbazole dendrimer groups linked to the core part through the 3,6-positions. Furthermore, tert-butyl groups are introduced into the molecular structure to occur good solubility. **36FCzG2** has glass transition temperature (T_g) = 162 °C, thermal decomposition temperature (T_d) = 461 °C, and the emission wavelength at 443 nm. Moreover, the highest occupied molecular orbital (HOMO) was 5.82 eV and the lowest unoccupied molecular orbital (LUMO) was 2.38 eV.

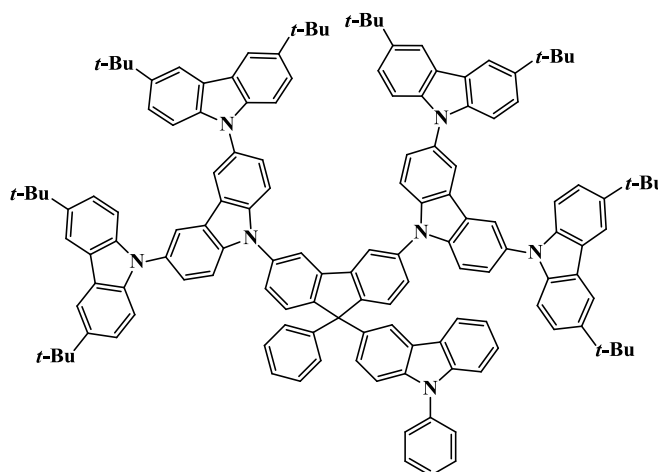


Figure 2.5 The structure of **36FCzG2** (Qian et al., 2013).

2.1.5 Cz-CBP

Yang and co-workers (2013) synthesized a dendritic host material 4,4-bis[3,6-bis(3,6-di-*tert*-butylcarbazol-9-yl)-carbazol-9-yl]-biphenyl or **Cz-CBP** by introduce of two 3,6-di-*tert*-butylcarbazole moieties into the 3, 6 position of the carbazole units to build a dendritic host material **Cz-CBP**. The glass transition temperature (T_g) was 287 °C and the emission wavelength at 402 nm. The structure was fabricated of ITO/PEDOT:PSS/Host:OXD-7(30 wt%):Flrpic(10 wt%)/Cs₂CO₃/Al was fabricated by solution-processing methods. Maximum current efficiency of 5.8 cd/A.

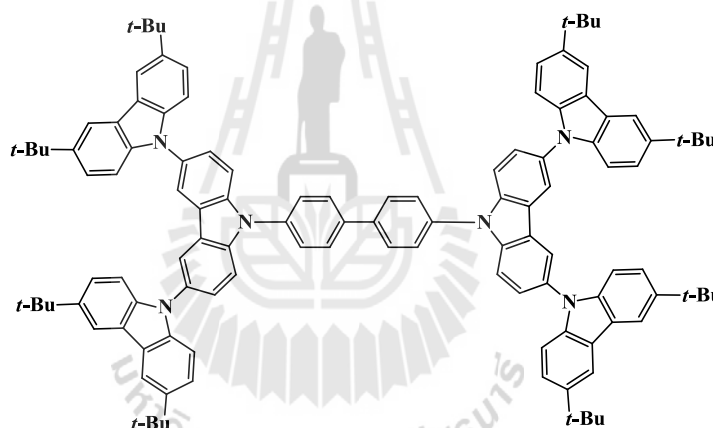


Figure 2.6 The structure of **Cz-CBP** (Yang et al., 2013).

2.1.6 CPMP

Deng and co-workers (2014) synthesized **CPMP** by introduction of pyrazole into the 3-position of the inner carbazole unit on one side. *tert*-Butyls are attached at the 3- and 6-sites of the outer carbazole rings to improve the solubility of these molecules. **CPMP** has emission wavelength at 401 nm, thermal decomposition temperature (T_d) was 424 °C, glass transition temperature (T_g) was 233 °C. Moreover,

the highest occupied molecular orbital (HOMO) was 5.30 eV, the lowest unoccupied molecular orbital (LUMO) was 2.18 eV, and the energy band gap (E_g) was 3.12 eV.

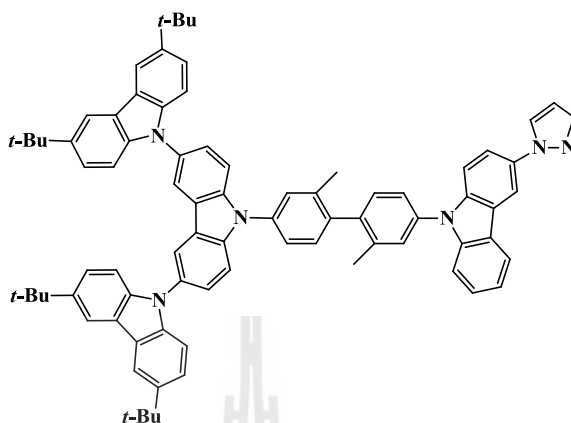


Figure 2.7 The structure of CPMP (Deng et al., 2014).

2.1.7 TPA-Cz

Singh and co-workers (2015) designed and synthesized **TPA-Cz** with triphenylamine as core and carbazole as peripheral group. Moreover, **TPA-Cz** reduced aggregation in solid state as well as improved thermal stability and solubility. **TPA-Cz** has emission wavelength at 433 nm and glass transition temperature (T_g) was 250 °C. The fluorescence quantum yield ($\Phi_f = 0.6$).

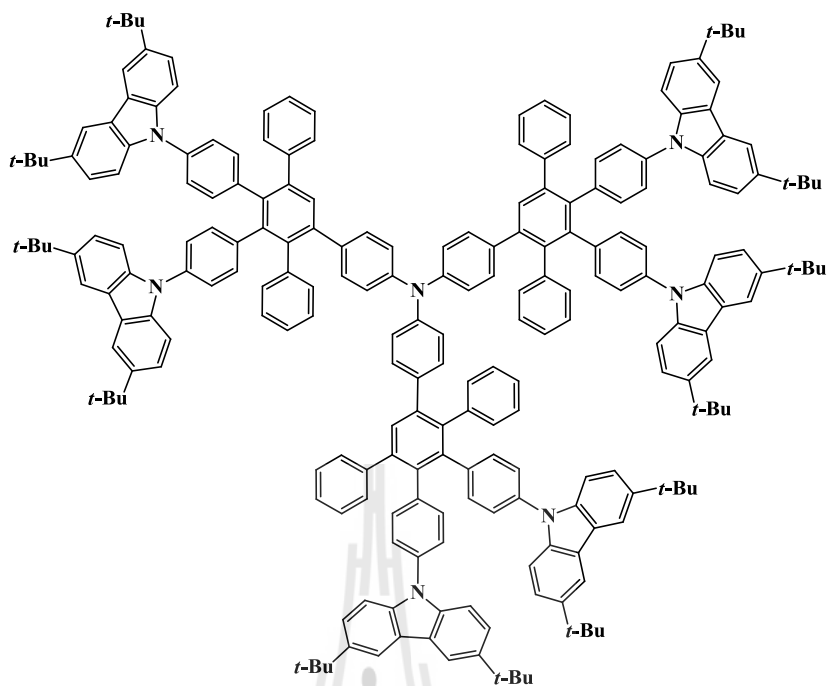


Figure 2.8 The structure of TPA-Cz (Singh et al., 2015).

2.1.8 G2F3

Zhang and co-workers (2015) synthesized the novel carbazole-based dendrimers, namely **G2F3** which has oligofluorene as core. Moreover, tert-butyl groups are introduced into the dendrimers surface to increase the solubility. The dendrimers are designed for excellent thermal and amorphous stability. **G2F3** has an emission wavelength at 407 nm, thermal decomposition temperature (T_d) was 440 °C, glass transition temperature (T_g) was 188 °C, and energy band gap (E_g) was 3.01 eV.

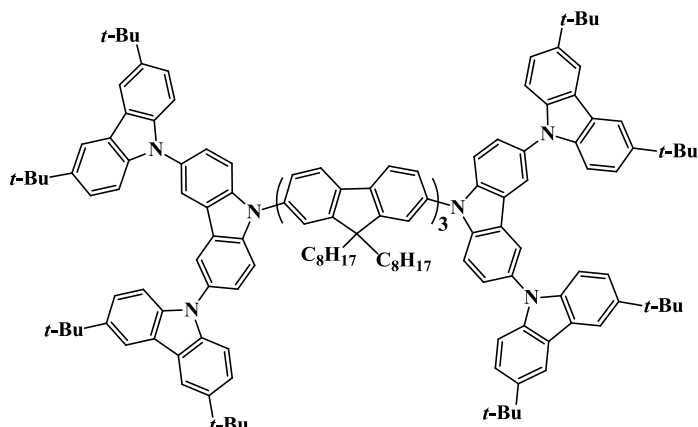


Figure 2.9 The structure of **G2F3** (Zhang et al., 2015).

According to the literature reviews, carbazole-containing organic molecules are among the most studied materials for hole-transporting layers due to their high hole mobility and good thermal stability. In this work, we designed bipolar 8-hydroxyquinoline derivative/carbazole dendrimers (G1-G2) to receive 8-hydroxyquinoline derivatives or (HQG1-HQG2) that possess electron transporting (8-hydroxyquinoline) and hole transporting (carbazole) properties. Furthermore, 8-hydroxyquinoline derivatives are very convenient and easy to be utilized in a device fabrication.

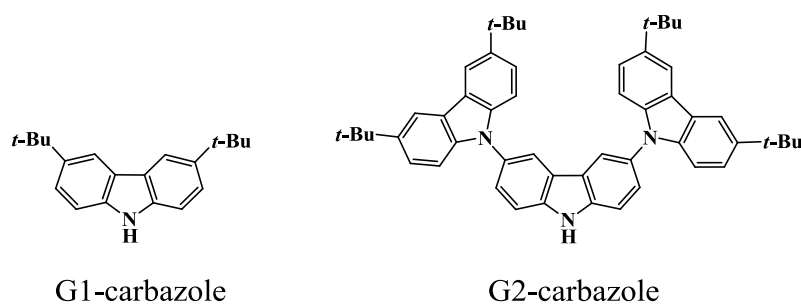


Figure 2.10 The structures of **G1-G2** carbazole.

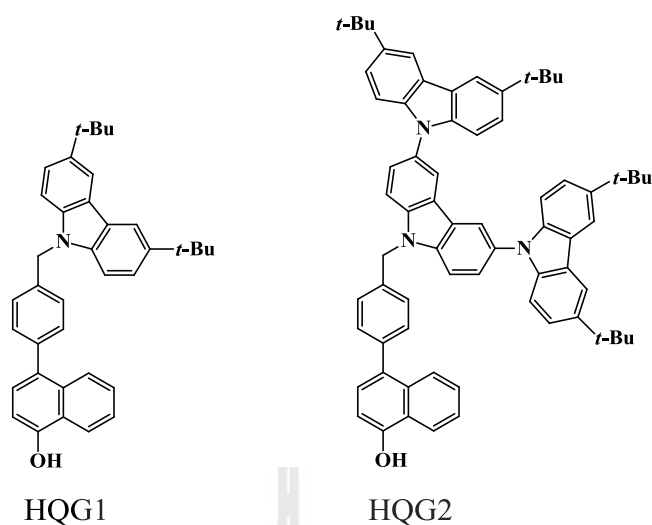


Figure 2.11 the structure of HQG1 and HQG2.

Research objectives

1. To synthesize ligand dendrimers with 8-hydroxyquinoline derivative and carbazole dendrimers (**G1-G2**) as 8-hydroxyquinoline derivatives (**HQG1**, and **HQG2**)
2. To characterize and identify the target molecules by $^1\text{H-NMR}$, $^{13}\text{C-NMR}$, Fourier transform infrared spectroscopy (FT-IR) and mass spectroscopic techniques
3. To study a photophysical and of 8-hydroxyquinoline derivatives under UV-Visible spectroscopy, and fluorescent spectroscopy and study thermal stability using DSC-TGA techniques.

CHAPTER III

EXPERIMENTS

3.1 Chemicals and reagents

All reagents and solvents will be used without further purification unless stated otherwise. Tetrahydrofuran (THF) was heated at reflux under nitrogen over sodium and benzophenone until the solution became blue and freshly distilled before use. Hexane, methylene chloride, acetyl acetate, methyl alcohol and ethyl alcohol were used to purify using column chromatography and crystallization. Column chromatography was carried out using silica gel (230-400 mesh) as stationary phase. CDCl_3 was used as solvents for $^1\text{H-NMR}$, $^{13}\text{C-NMR}$ and methylene chloride as solvent for UV-Visible spectroscopy and fluorescence spectroscopy.

3.2 Characterization techniques

Chemical structure of all molecules was identified by means of $^1\text{H-NMR}$ and $^{13}\text{C-NMR}$, and functional groups were verified by Fourier Transform Infrared (FT-IR) technique. The molecular weight of all molecules was certified by mass spectroscopy. The optical property of target molecules was determined by UV-visible spectroscopy. Thermal property was monitored by Differential Scanning Calorimetry (DSC) and Thermogravimetric Analysis (TGA).

3.2.1 Nuclear magnetic resonance (NMR)

Bruker AVANCE 500 MHz was used for study the chemical structure of target molecules. The CDCl_3 solvent was used for dissolve the target molecule and using TMS (0.00 ppm) as an internal reference. The chemical shift (δ ppm), multiplicity and integration (Hz) were used to represent NMR information.

3.2.2 Fourier Transform Infrared Spectroscopy (FT-IR)

Perkin-Elmer can give FT-IR spectra after the mixture of (sample 1: KBr 10). The FT-IR data was shown as wavenumber (cm^{-1}) and % Transmittance (%T).

3.2.3 UV-Visible spectroscopy

Perkin Elmer, Lambda 750S can present UV-visible spectra. The sample was dissolved in dried organic solvent and diluted solutions, respectively. The sample was poured in quartz tube and then examined.

3.2.4 Differential scanning calorimetry (DSC) and thermo gravimetric analysis (TGA)

The thermal properties were investigated by TGA Instrument/ SDT2960 which can give the DSC-TGA spectra. 10 mg of sample was put into an alumina pan that was placed to the TGA balance.

3.2.5 Mass spectroscopy

JEOL, JMS-700 was used record mass spectra. The sample was dissolved in dried organic solvents and dropped in plate.

3.2.6 Melting point (m.p.)

Melting point was measured by Buchi 530 in a capillary tube under O_2 at a heating rate $20\text{ }^\circ\text{C}/\text{min}$.

3.2.7 Fluorescence spectroscopy

Perkin-Elmer luminescence spectrometer can present photoluminescence spectra after dissolution of sample in a dried organic solution system.

3.3 Experimental

3.3.1 5-Bromo-8-tosylquinoline (2)

A mixture of 5-bromo-8-hydroxyquinoline (1.00 g, 4.46 mmol), NaOH (0.98 g, 24.55 mmol), *p*-toluenesulfonyl chloride (0.94 g, 4.93 mmol) in acetone (50 mL) was refluxed under N₂ atmosphere for 3 h (Heiskanen and Hormi, 2009). After the mixture was cooled to room temperature, water (50 mL) was added. The mixture was then extracted with CH₂Cl₂ (100 mL x 2). The combined organic layer was washed with water (50 mL), brine solution (50 mL) and dried over anhydrous Na₂SO₄. The solvent was removed to obtain crude product. The crude product was finally purified by crystallization using the mixture of CH₂Cl₂ and methanol to afford a brown solid product. Yield 95% (1.60 g); m.p.: 145.0-146.0 °C; ¹H-NMR (500 MHz, CDCl₃) δ 8.926 (1H, d, *J* = 4.25 Hz), 8.583 (1H, d, *J* = 8.5 Hz), 7.961 (2H, d, *J* = 8.5 Hz), 7.884 (1H, d, *J* = 8.5 Hz), 7.608-7.563 (2H, m), 7.366 (2H, d, *J* = 8.5 Hz), 2.512 (3H, s) ppm. ¹³C-NMR (125 MHz, CDCl₃) δ 151.32, 145.27, 142.33, 135.52, 132.98, 129.63, 129.55, 128.81, 128.78, 122.95, 122.89, 120.27, 21.71 ppm; MALDI-TOF *m/z*: 379.97, Calcd for C₁₅H₁₂SO₃NBr: 378.24; IR (KBr): 3400, 1589, 1459, 1371, 1290, 1173, 1050, 785, 667 cm⁻¹.

3.3.2 5-(4-(Hydroxymethyl)phenyl)-8-tosylquinoline (3)

A mixture of **2** (1.60 g, 4.21 mmol), 4-(hydroxymethyl)phenylboronic acid (0.70 g, 4.65 mmol), Pd(PPh₃)₄ (0.10 g, 0.08 mmol) and 2M Na₂CO₃ (42.11 mL,

84.21 mmol) in THF (80 mL) was purged with N₂ (Heiskanen and Hormi, 2009). The reaction was refluxed under N₂ atmosphere for 24 h. After the mixture was cooled to room temperature, water (50 mL) was added. The mixture was extracted with CH₂Cl₂ (50 mL x 2). The combined organic layer was washed with water (50 mL), brine solution (50 mL), and dried over anhydrous Na₂SO₄. The crude product was purified by column chromatography using silica gel eluting with a mixture of CH₂Cl₂ and hexane to afford a white solid product. Yield 95% (1.62 g); m.p.: 152.0-153.0 °C ; ¹H-NMR (500 MHz, CDCl₃) δ 8.921 (1H, d, *J* = 4 Hz), 8.265 (1H, d, *J* = 8.5 Hz), 8.028 (2H, d, *J* = 8.5 Hz), 7.693 (1H, d, *J* = 8.0 Hz), 7.606 (2H, d, *J* = 8.0 Hz), 7.532-7.507 (3H, m), 7.433 (1H, t, *J* = 4.0, 5.0 Hz), 7.393 (2H, d, *J* = 8.0 Hz), 4.904 (2H, s), 2.524(3H, s) ppm; ¹³C-NMR (125 MHz, CDCl₃) δ 150.55, 145.06, 140.67, 139.43, 137.92, 134.27, 130.21, 129.53, 128.81, 128.00, 127.20, 126.57, 121.89, 121.75, 65.04, 21.72 ppm; MALDI-TOF *m/z*: 406.15, Calcd for C₂₂H₁₉SO₄N: 405.47; IR (KBr): 3560, 3400, 1340, 1174, 1046, 782 cm⁻¹.

3.3.3 5-(4-(Chloromethyl)phenyl)-8-tosylquinoline (4)

A mixture of **3** (1.62 g, 3.99 mmol) and thionyl chloride (1.45 mL, 19.96 mmol) in THF (20 mL) was refluxed under N₂ atmosphere for 4 h (Robert et al., 1958). After the mixture was cooled to room temperature, Na₂CO₃ (2 M, 8.0 mL) was added. The mixture was extracted with CH₂Cl₂ (50 mL x 2). The combined organic layer was washed with water (20 mL), brine solution (20 mL) and dried over anhydrous Na₂SO₄. The crude product was purified by column chromatography using silica gel eluting with the mixture of CH₂Cl₂ and hexane to afford a yellow solid product. Yield 97% (1.64 g); m.p.: 141.0-142.0 °C; ¹H-NMR (500 MHz, CDCl₃) δ 8.931 (1H, d, *J* = 4 Hz), 8.252 (1H, d, *J* = 8.5 Hz), 8.028 (2H, d, *J* = 8.0 Hz), 7.70

(1H, d, $J = 8.0$ Hz), 7.626 (2H, d, $J = 8.0$ Hz), 7.529-7.510 (3H, m), 7.444 (1H, t, $J = 4.0, 5.0$ Hz), 7.395 (2H, d, $J = 8.0$ Hz), 4.780 (2H, s), 2.525 (3H, s) ppm; ^{13}C -NMR (125 MHz, CDCl_3) δ 150.61, 145.12, 145.04, 141.79, 139.03, 138.68, 137.33, 134.19, 133.42, 130.37, 130.17, 129.56, 128.86, 128.80, 127.91, 126.62, 121.88, 121.85, 45.87, 21.73 ppm; MALDI-TOF m/z : 424.09. Calcd for $\text{C}_{22}\text{H}_{18}\text{SO}_3\text{NCl}$: 423.91; IR (KBr): 3402, 1593, 1369, 1170, 1051, 781, 588 cm^{-1} .

3.3.4 5-(4-((G1)Methyl)phenyl)-8-tosylquinoline (HQOTsG1)

The carbazole G1-carbazole (0.42 g, 1.61 mmol) was dissolved by using dimethylformamide (DMF) 20 mL after that NaH (0.05 g, 2.35 mmol) was added into the reaction and stirred in ice bath for 30 min, respectively. The **compound 4** (0.50 g, 1.17 mmol) was added in this reaction and refluxed under N_2 atmosphere for 6 h (Wang et al., 2008). After the reaction was cooled to room temperature, HCl (1 M, 2.4 mL) was added. The mixture was extracted with CH_2Cl_2 (50 mL x 2). The combined organic layer was washed with water (20 mL), brine solution (20 mL) and dried over anhydrous Na_2SO_4 . The crude product was purified by column chromatography using silica gel eluting with the mixture of ethyl acetate and hexane to afford a yellow solid product. Yield 89% (0.70 g); m.p.: 136.0-137.0 $^\circ\text{C}$; ^1H -NMR (500 MHz, CDCl_3) δ 8.843 (1H, d, $J = 4$ Hz), 8.190 (2H, s), 8.154 (1H, d, $J = 8.5$ Hz), 7.949 (2H, d, $J = 8.0$ Hz), 7.601 (1H, d, $J = 7.5$ Hz), 7.548 (2H, d, $J = 8.5$ Hz), 7.413-7.288 (10H, m), 5.580 (2H, s), 2.447 (3H, s), 1.501 (18H, s) ppm; ^{13}C -NMR (125 MHz, CDCl_3) δ 150.51, 145.05, 144.84, 142.17, 141.71, 139.29, 139.18, 137.61, 137.60, 134.35, 133.42, 130.35, 129.52, 128.79, 127.92, 126.85, 126.55, 123.59, 122.99, 121.87, 121.71, 116.47, 108.20, 46.46, 32.08, 21.71 ppm; MALDI-TOF m/z : 666.3; Calcd for

$C_{42}H_{42}SO_3N_2$: 666.87; IR (KBr): 3401, 2950, 2857, 1594, 1476, 1359, 1295, 1173, 1049, 782 cm^{-1} .

3.3.5 5-(4-((G1)Methyl)phenyl)-8-hydroxyquinoline (HQG1)

A mixture of **HQOTsG1** (0.70 g, 1.00 mmol) and 1M NaOH (3.00 ml, 3.01 mmol) in THF:DMSO:H₂O (10 mL:5 mL:3 mL) was refluxed under N₂ atmosphere for 3 h (Heiskanen and Hormi, 2009). After the mixture was cooled to room temperature, HCl (1 M, 3.00 mL) was added. The mixture was extracted with CH₂Cl₂ (50 mL x 2). The combined organic layer was washed with water (20 mL), brine solution (20 mL) and dried over anhydrous Na₂SO₄. The solvent was removed to obtain crude product. The crude product was finally purified by crystallization using the mixture of CH₂Cl₂, hexane and methanol to afford a yellow solid product. Yield 98% (0.53 g); m.p.: 220.0-221.0 °C; ¹H-NMR (500 MHz, CDCl₃) δ 8.863 (1H, d, *J* = 4 Hz), 8.312 (1H, d, *J* = 8.5 Hz), 7.253 (2H, s), 7.616 (2H, d, *J* = 8.5 Hz), 7.478-7.356 (8H, m), 7.294 (1H, d, *J* = 8.0 Hz), 5.642 (2H, s), 1.567 (18H, s) ppm; ¹³C-NMR (125 MHz, CDCl₃) δ 151.57, 147.51, 142.08, 139.22, 138.44, 136.74, 134.91, 130.44, 128.35, 126.78, 126.70, 123.56, 122.96, 121.75, 116.43, 109.68, 108.24, 46.51, 32.08 ppm; MALDI-TOF *m/z*: 512.30, Calcd for C₃₆H₃₆ON₂: 512.68; IR (KBr): 3396, 2946, 2855, 1581, 1476, 1363, 1263, 789 cm^{-1} .

3.3.6 5-(4-((G2)Methyl)phenyl)-8-tosylquinoline (HQOTsG2)

The carbazole G2-carbazole (1.27 g, 1.76 mmol) was dissolved by using tetrahydrofuran (THF) after that NaH (0.05 g, 2.35 mmol) was added into the reaction and stirred in ice bath for 30 min, respectively. The **compound 4** (0.50 g, 1.17 mmol) was added in this reaction and refluxed under N₂ atmosphere for 6 h (Wang et al., 2008). After the reaction was cooled to room temperature, HCl (1 M, 2.4 mL) was

added. The mixture was extracted with CH_2Cl_2 (50 mL x 2). The combined organic layer was washed with water (20 mL), brine solution (20 mL) and dried over anhydrous Na_2SO_4 . The crude product was purified by column chromatography using silica gel eluting with the mixture of ethyl acetate and hexane to afford a white solid product. Yield 85% (1.11 g); m.p.: 268.0-269.0 °C; $^1\text{H-NMR}$ (500 MHz, CDCl_3) δ 8.965 (1H, d, $J = 3$ Hz), 8.350 (2H, s), 8.309 (1H, d, $J = 8$ Hz), 8.260 (4H, s), 8.048 (2H, d, $J = 8.5$ Hz), 7.768 (4H, m), 7.565-7.538 (11H, m), 7.480-7.391 (6H, m), 5.889 (2H, s), 2.528 (3H, s), 1.561 (36H, s) ppm; $^{13}\text{C-NMR}$ (125 MHz, CDCl_3) δ 150.53, 142.60, 140.17, 140.15, 139.08, 136.65, 130.70, 130.51, 129.55, 128.83, 127.94, 126.84, 126.01, 123.75, 123.56, 123.13, 121.84, 119.56, 116.24, 110.14, 109.08, 46.87, 32.05, 21.73 ppm; MALDI-TOF m/z : 1109.30, Calcd for $\text{C}_{74}\text{H}_{72}\text{SO}_3\text{N}_4$: 1109.46; IR (KBr): 3401, 2948, 2856, 1489, 1360, 1287, 1172, 1048, 805 cm^{-1} .

3.3.7 5-(4-((G2)Methyl)phenyl)-8-hydroxyquinoline (HQG2)

A mixture of **HQOTsG2** (1.11 g, 0.38 mmol) and 1M NaOH (3.00 mL, 3.00 mmol) in THF:DMSO:H₂O (10mL:5mL:3mL) was refluxed under N₂ atmosphere for 3 h (Heiskanen and Hormi, 2009). After the mixture was cooled to room temperature, HCl (1 M, 3.00 mL) was added. The mixture was extracted with CH_2Cl_2 (50 mL x 2). The combined organic layer was washed with water (20 mL), brine solution (20 mL) and dried over anhydrous Na_2SO_4 . The solvent was removed to obtain crude product. The crude product was finally purified by crystallization using a mixture CH_2Cl_2 , hexane and methanol to afford a white solid product. Yield 98% (0.94 g); m.p.: 294.0-295.0 °C; $^1\text{H-NMR}$ (500 MHz, CDCl_3) δ 8.900 (1H, d, $J = 3$ Hz), 8.412 (1H, d, $J = 8.5$), 8.343 (2H, s), 8.255 (4H, s), 7.774 (4H, d, $J = 8.5$), 7.588-7.519 (11H, m), 7.433

(4H, d, $J = 8.5$), 5.883 (2H, s), 1.557 (36H, s) ppm; ^{13}C -NMR (125 MHz, CDCl_3) δ 142.57, 140.19, 130.78, 130.45, 126.81, 125.99, 123.72, 123.55, 123.12, 119.53, 116.23, 110.19, 109.10, 46.98, 32.09 ppm; MALDI-TOF m/z : 955.78, Calcd for $\text{C}_{68}\text{H}_{66}\text{ON}_4$: 955.28; IR (KBr): 3405, 2948, 2894, 1577, 1488, 1361, 1261, 806 cm^{-1} .



CHAPTER IV

RESULTS AND DISCUSSION

4.1 Synthesis

The target materials **HQG1** and **HQG2** were synthesized as outlined in Figure 4.1. A mixture of compound **1** and *p*-toluenesulfonyl chloride under tosylation reaction in the presence of sodium hydroxide as base in acetone provided compound **2**. Coupling of compound **2** with an excess of 4-(hydroxymethyl)phenylboronic acid under Suzuki-cross coupling reaction in the presence of Pd(PPh₃)₄ and sodium carbonate, as a catalyst and base, respectively. The reaction was refluxed in tetrahydrofuran under nitrogen atmosphere which gave compound **3**. Chlorination of compound **3** with thionyl chloride in tetrahydrofuran gave compound **4**. A mixture of compound **4** and Gn-carbazole under substitution reaction in the presence of sodium hydride as base in dimethylformamide and tetrahydrofuran gave **HQOTsG1** and **HQOTsG2**. Detosylation of **HQOTsG1** and **HQOTsG2** with sodium hydroxide in THF:DMSO:H₂O selectively produced the corresponding **HQG1** and **HQG2** in good yield. The target materials **HQG1** and **HQG2** were purified by crystallization from a mixture of dichloromethane hexane and methanol to give yellow solids and white solids.

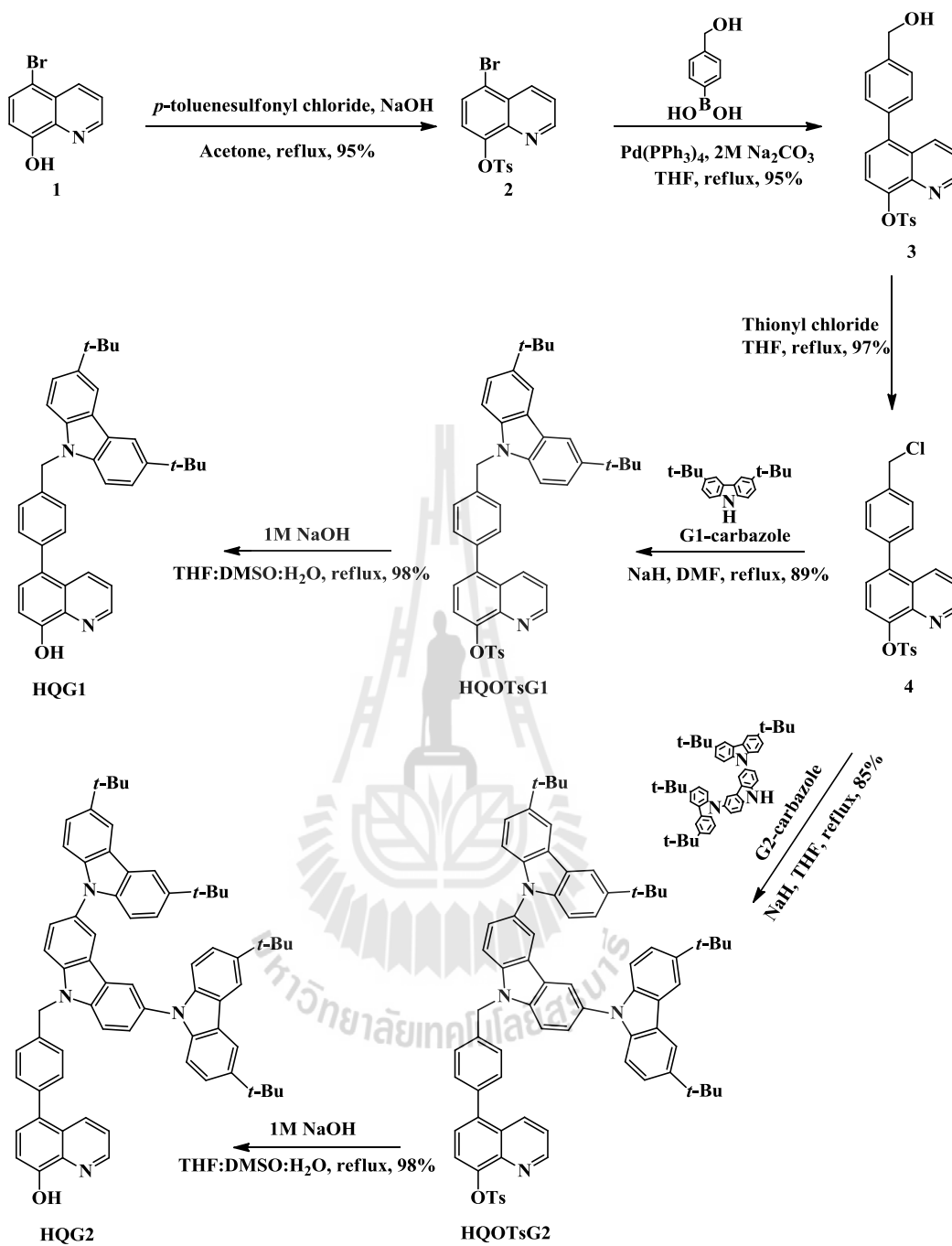


Figure 4.1 Synthesis of hole-transporting materials **HQG1** and **HQG2** for OLEDs.

4.1.1 5-Bromo-8-tosylquinoline (2)

The synthesis of a **compound 2** is outlined in **Figure 4.2**. The **compound 2** was synthesized by reaction of **compound 1**, *p*-toluenesulfonyl chloride and sodium hydroxide in acetone. The reaction was refluxed to afford the **compound 2** as a brown solid in 95% yield. The chemical structure of **compound 2** was confirmed by mass spectrometry and ¹H-NMR. Mass spectrometry gave MALDI-TOF *m/z*: 379.97, Calcd for C₁₅H₁₂SO₃NBr: 378.24. The ¹H-NMR spectrum of **compound 2** composed of the doublet four peaks at chemical shift 8.926, 8.583, 7.884, 7.572 ppm (4H), and the triplet peak at chemical shift 7.608-7.590 ppm (1H) assigning as the protons of quinoline ring. Finally, the doublet of doublet two peaks at chemical shift 7.961 and 7.366 ppm (4H), and the singlet peak at chemical shift 2.512 ppm (3H) assigning as the protons of tosyl group. The **compound 2** was soluble in dichloromethane solvent at room temperature.

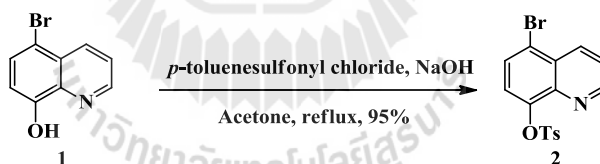


Figure 4.2 The synthesis of **compound 2**.

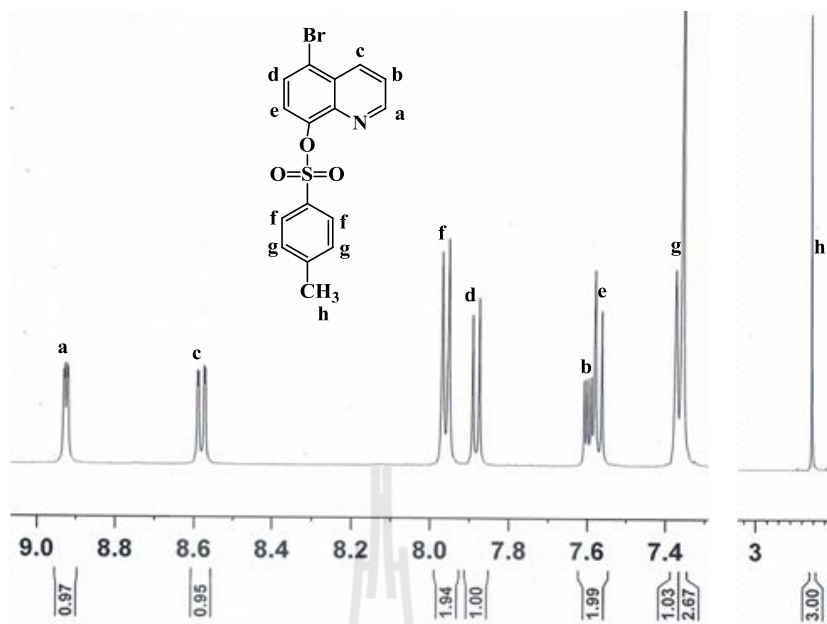


Figure 4.3 $^1\text{H-NMR}$ of compound 2 in CDCl_3 .

4.1.2 5-(4-(Hydroxymethyl)phenyl)-8-tosylquinoline (3)

The synthesis of a **compound 3** is outlined in **Figure 4.4**. The **compound 2** was synthesized by reaction of **compound 2**, 4-(hydroxymethyl)phenylboronic acid, $\text{Pd}(\text{PPh}_3)_4$ and $2\text{M Na}_2\text{CO}_3$ in tetrahydrofuran (THF). The reaction was refluxed to afford the **compound 3** as a white solid in 95% yield. The chemical structure of **compound 3** was confirmed by mass spectroscopy and $^1\text{H-NMR}$. Mass spectrometry gave MALDI-TOF m/z : 406.15, Calcd for $\text{C}_{22}\text{H}_{19}\text{SO}_4\text{N}$: 405.47. The $^1\text{H-NMR}$ spectrum of **compound 3** composed of the doublet four peaks at chemical shift 8.921, 8.265, 7.693, 7.528 ppm (4H) and the triplet peak at chemical shift 7.456-7.430 ppm (1H) assigning as the protons of quinoline ring. The doublet of doublet two peaks at chemical shift 8.028 and 7.393 ppm (4H) and the singlet peak at chemical shift 2.524 ppm (3H) assigning as the protons of tosyl group. The doublet of doublet two peaks at chemical shift 7.606 and 7.512 ppm (4H) assigning as the protons of phenyl ring.

Finally, the singlet peak at chemical shift 4.904 ppm (2H) assigning as the protons of methyl group. The **compound 3** was soluble in dichloromethane solvent at room temperature.

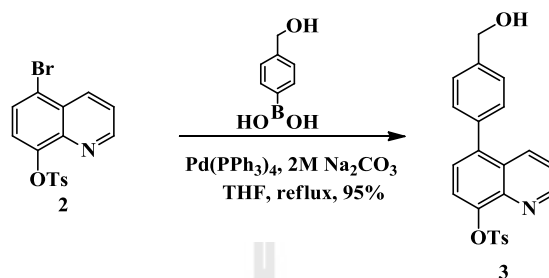


Figure 4.4 The synthesis of **compound 3**.

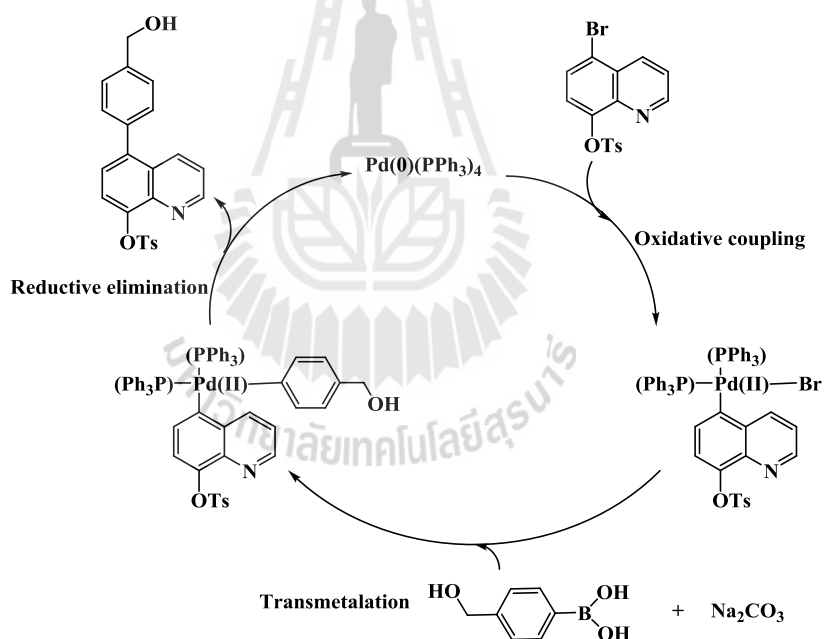


Figure 4.5 Generally accepted mechanism for Suzuki reaction in a homogeneous phase.

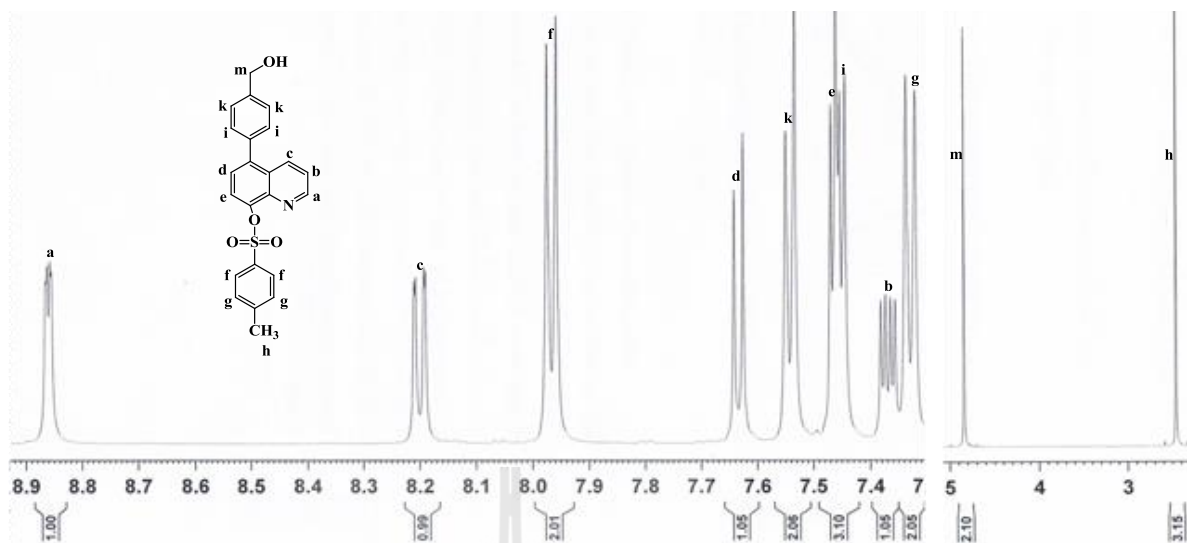


Figure 4.6 $^1\text{H-NMR}$ of compound **3** in CDCl_3 .

4.1.3 5-(4-(Chloromethyl)phenyl)-8-tosylquinoline (**4**)

The synthesis of a **compound 4** is outlined in **Figure 4.7**. The **compound 4** was synthesized by reaction of **compound 3** and thionyl chloride in tetrahydrofuran (THF). The reaction was refluxed to afford the **compound 4** as a yellow solid in 97% yield. The chemical structure of **compound 4** was confirmed by mass spectroscopy and $^1\text{H-NMR}$. Mass spectrometry gave MALDI-TOF m/z : 424.09. Calcd for $\text{C}_{22}\text{H}_{18}\text{SO}_3\text{NCl}$: 423.91. The $^1\text{H-NMR}$ spectrum of **compound 4** composed of the doublet four peaks at chemical shift 8.931, 8.252, 7.700, 7.528 ppm (4H) and the triplet peak at chemical shift 7.456-7.430 ppm (1H) assigning as the protons of quinoline ring. The doublet of doublet two peaks at chemical shift 8.028 and 7.395 ppm (4H) and the singlet peak at chemical shift 2.525 ppm (3H) assigning as the protons of tosyl group. The doublet of doublet two peaks at chemical shift 7.626 and 7.512 ppm (4H) assigning as the protons of phenyl ring. Finally, the singlet peak at

chemical shift 4.780 ppm (2H) assigning as the protons of methyl group. The **compound 4** was soluble in dichloromethane solvent at room temperature.

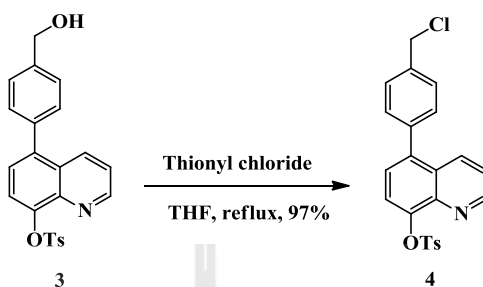
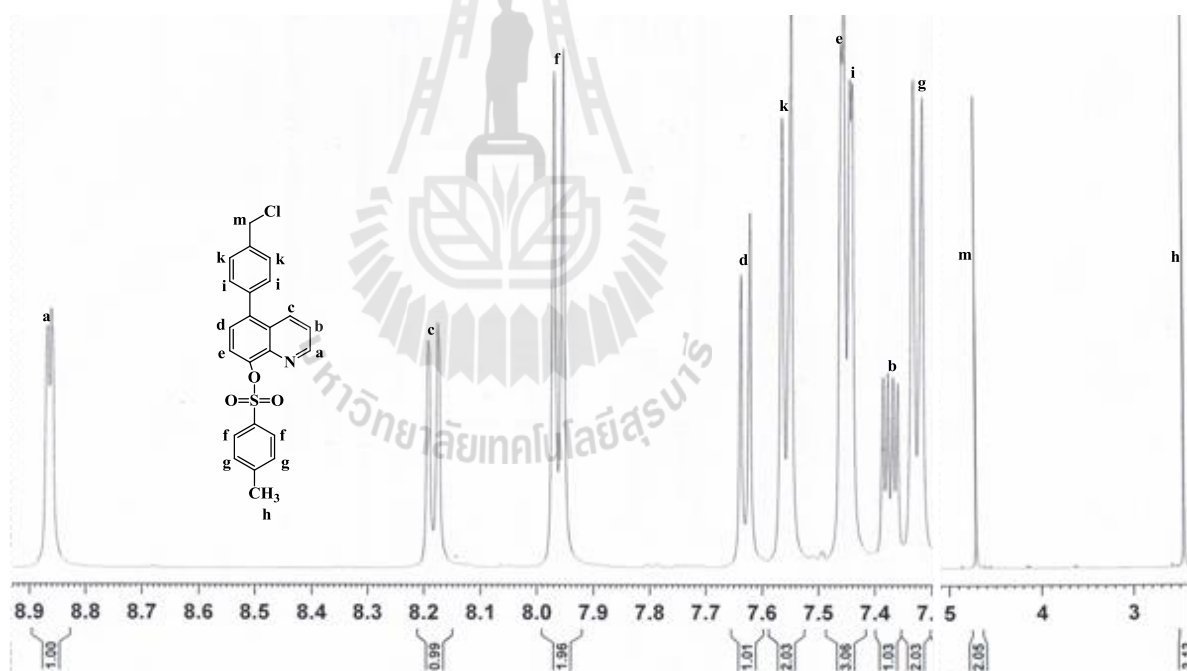


Figure 4.7 The synthesis of **compound 4**.



4.1.4 5-(4-((G1)Methyl)phenyl)-8-tosylquinoline (HQOTsG1)

The synthesis of **HQOTsG1** is outlined in **Figure 4.9**. The **HQOTsG1** was synthesized by reaction of **compound 4**, G1-carbazole, and sodium hydride in

dimethylformamide (DMF). The reaction was heat at 60 °C to afford **HQOTsG1** as a yellow solid in 89% yield. The chemical structure of **HQOTsG1** was confirmed by mass spectroscopy and ¹H-NMR. Mass spectrometry gave MALDI-TOF*m/z*: 666.30; Calcd for C₄₂H₄₂SO₃N₂: 666.87. The ¹H-NMR spectrum of **HQOTsG1** composed of the doublet three peaks at chemical shift 8.843, 8.154, 7.601 ppm (3H) assigning as the protons of quinoline ring. The doublet of doublet peak at chemical shift 7.949 ppm (2H) and the singlet peak at chemical shift 2.447 ppm (3H) assigning as the protons of tosyl group. The singlet peak at chemical shift 8.190 ppm (2H), the doublet of doublet peak at chemical shift 7.548 ppm (2H), and the singlet peak at chemical shift 1.501 ppm (18H) assigning as the protons of G1-carbazole. Finally, the singlet peak at chemical shift 5.580 ppm (2H) assigning as the protons of methyl group. **HQOTsG1** was soluble in dichloromethane solvent at room temperature.

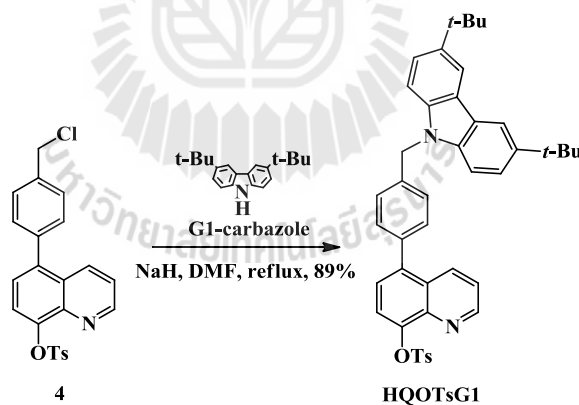


Figure 4.9 The synthesis of **HQOTsG1**.

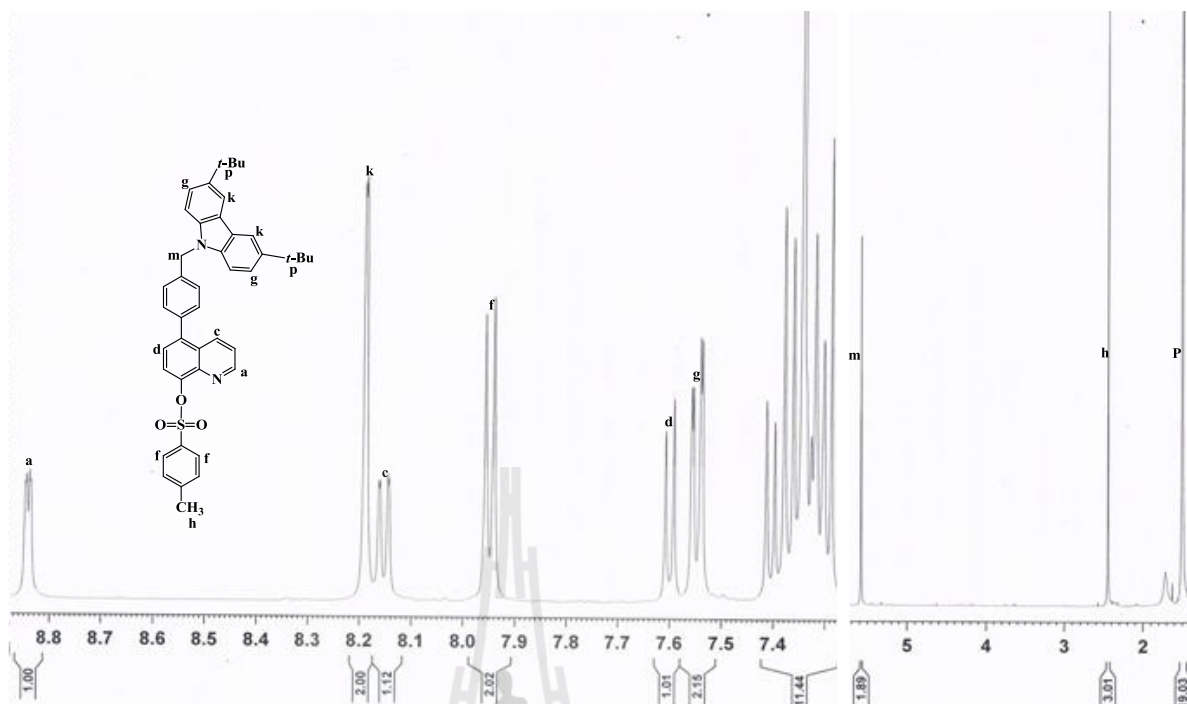


Figure 4.10 $^1\text{H-NMR}$ of **HQOTsG1** in CDCl_3 .

4.1.5 5-(4-((G1)Methyl)phenyl)-8-hydroxyquinoline (**HQG1**)

The synthesis of **HQG1** is outlined in **Figure 4.11**. The **HQG1** was synthesized by reaction of **HQOTsG1** and aqueous solution of 1M NaOH in THF:DMSO:H₂O. The reaction was refluxed to afford **HQG1** as a yellow solid in 98% yield. The chemical structure of **HQG1** was confirmed by mass spectroscopy and $^1\text{H-NMR}$. Mass spectrometry gave MALDI-TOF m/z : 512.30, Calcd for $\text{C}_{36}\text{H}_{36}\text{ON}_2$: 512.68. The $^1\text{H-NMR}$ spectrum of **HQG1** composed of the doublet two peaks at chemical shift 8.863 and 8.320 ppm (2H) assigning as the protons of quinoline ring. The singlet peak at chemical shift 8.252 ppm (2H), the doublet peak at chemical shift 7.615 ppm (2H), and the singlet peak at chemical shift 1.567 ppm (18H) assigning as the protons of G1-carbazole. Finally, the singlet peak at chemical

shift 5.642 ppm (2H) assigning as the protons of methyl group. **HQG1** is soluble in dichloromethane solvent at room temperature.

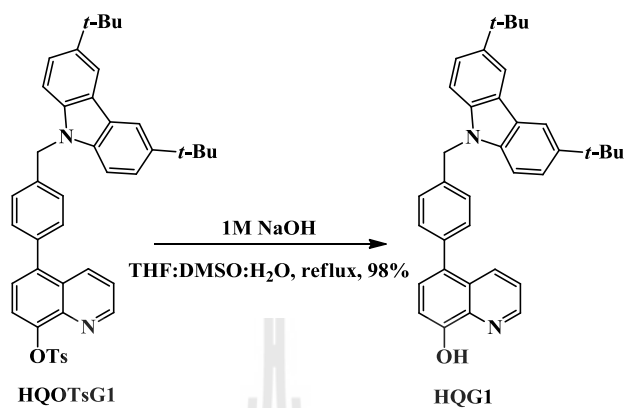


Figure 4.11 The synthesis of **HQG1**.

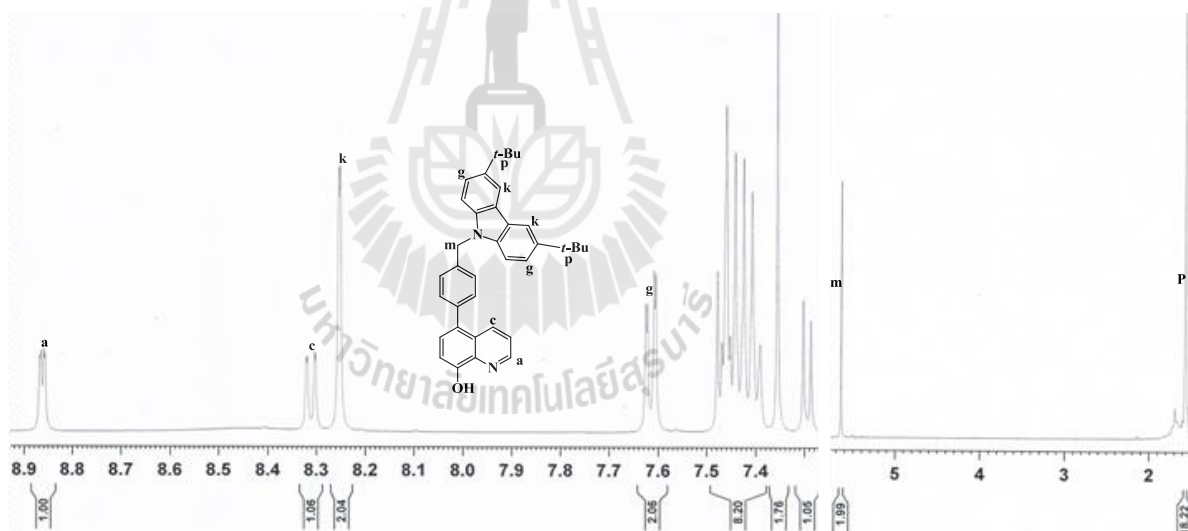


Figure 4.12 ¹H-NMR of **HQG1** in CDCl₃.

4.1.6 5-(4-((G2)Methyl)phenyl)-8-tosylquinoline (HQOTsG2)

The synthesis of **HQOTsG2** is outlined in **Figure 4.13**. The **HQOTsG2** was synthesized by reaction of **compound 4**, G2-carbazole, and sodium hydride in tetrahydrofuran (THF). The reaction was refluxed to afford **HQOTsG2** as a white solid in 85% yield. The chemical structure of **HQOTsG2** was confirmed by mass spectroscopy and $^1\text{H-NMR}$. Mass spectrometry gave MALDI-TOF m/z : 1109.01, Calcd for $\text{C}_{74}\text{H}_{72}\text{SO}_3\text{N}_4$:1109.46. The $^1\text{H-NMR}$ spectrum of **HQOTsG2** composed of the doublet two peaks at chemical shift 8.965 and 8.309 ppm (2H) assigning as the protons of quinoline ring. The doublet of doublet peak at chemical shift 8.048 ppm (2H) and the singlet peak at chemical shift 2.528 ppm (3H) assigning as the protons of tosyl group. The singlet two peaks at chemical shift 8.350 ppm (2H) and 8.260 ppm (4H), the doublet peak at chemical shift 7.768 ppm (4H), and the singlet peak at chemical shift 1.561 ppm (36H) assigning as the protons of G2-carbazole. Finally, the singlet peak at chemical shift 5.889 ppm (2H) assigning as the protons of methyl group. **HQOTsG2** is soluble in dichloromethane solvent at room temperature.

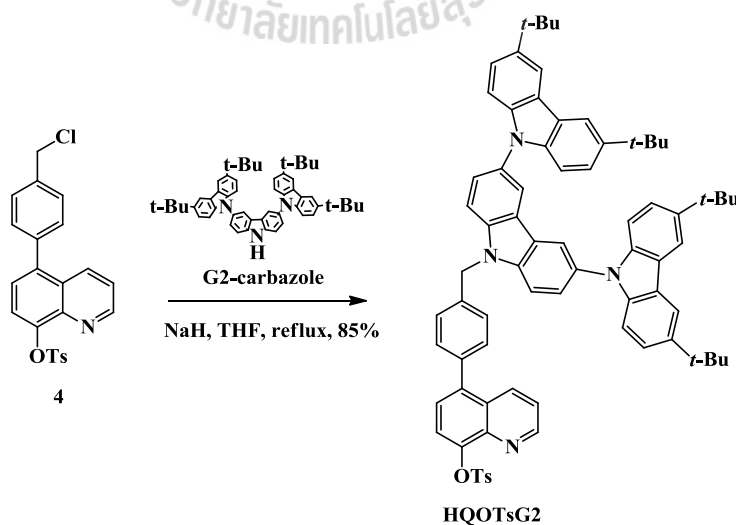


Figure 4.13 The synthesis of **HQOTsG2**.

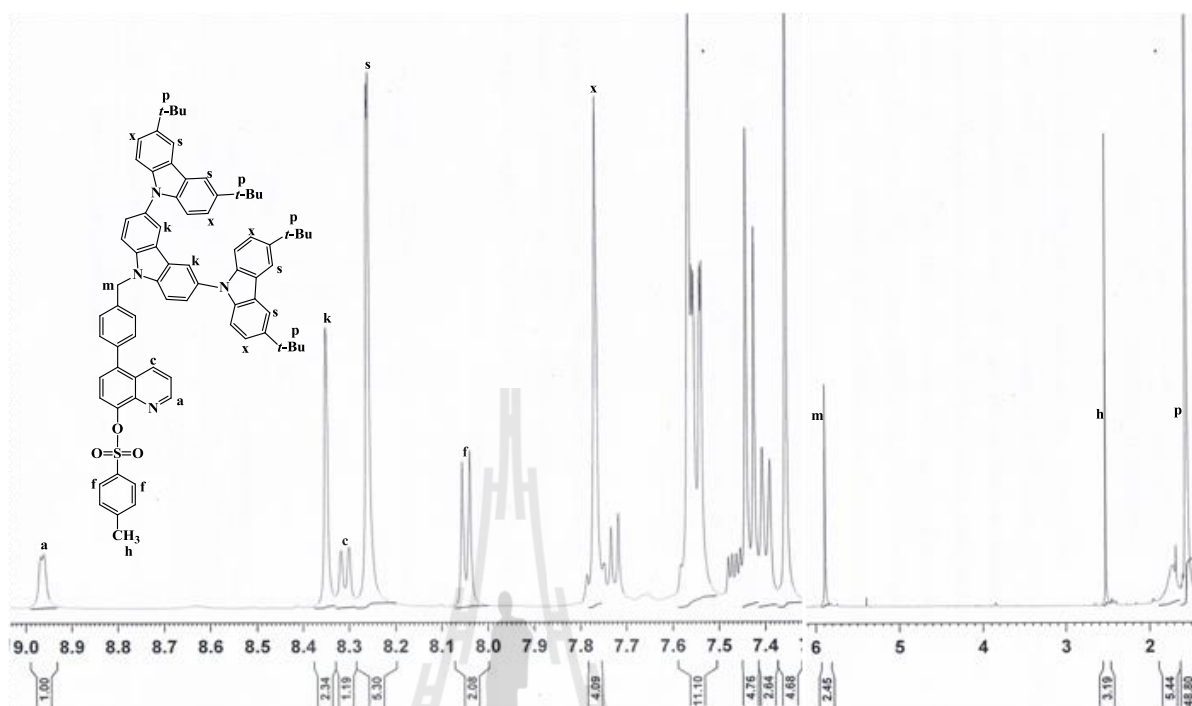


Figure 4.14 ¹H-NMR of HQOTsG2 in CDCl₃.

4.1.7 5-(4-((G2)Methyl)phenyl)-8-hydroxyquinoline (HQG2)

The synthesis of HQG2 is outlined in Figure 4.15. The HQG2 was synthesized by reaction of HQOTsG2 and aqueous solution of 1M NaOH in THF:DMSO:H₂O. The reaction was refluxed to afford HQG2 as a white solid in 98% yield. The chemical structure of HQG2 was confirmed by mass spectroscopy and ¹H-NMR. Mass spectrometry gave MALDI-TOF *m/z*: 955.78, Calcd for C₆₈H₆₆ON₄: 955.28. The ¹H-NMR spectrum of HQG2 composed of the doublet two peaks at chemical shift 8.900 and 8.412 ppm (2H) assigning as the protons of quinoline ring. The singlet two peaks at chemical shift 8.343 ppm (2H) and 8.254 ppm (4H), the doublet two peaks at chemical shift 7.768 ppm (4H) and 7.432 ppm (4H), and the singlet peak at chemical shift 1.557 ppm (36H) assigning as the protons of G2-

carbazole. Finally, the singlet peak at chemical shift 5.883 ppm (2H) assigning as the protons of methyl group. **HQG2** is soluble in dichloromethane solvent at room temperature.

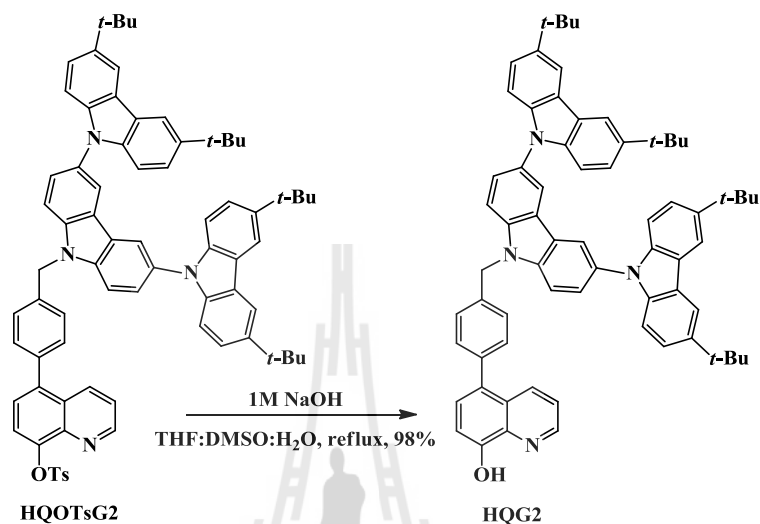


Figure 4.15 The synthesis of **HQG2**.

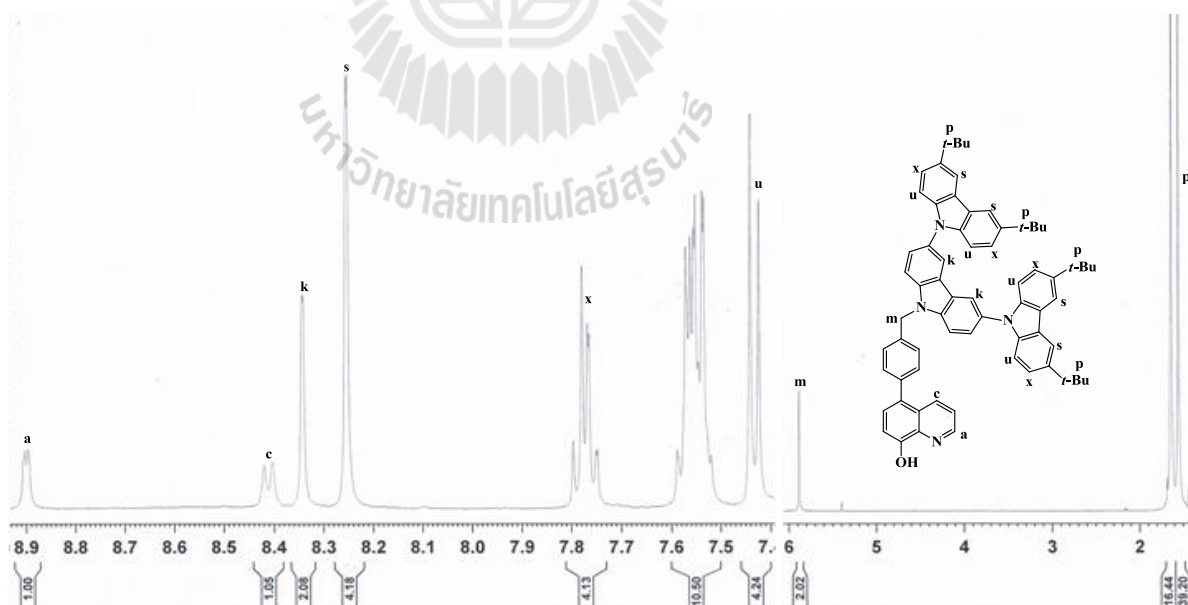


Figure 4.16 $^1\text{H-NMR}$ of **HQG2** in CDCl_3 .

4.2 Optical properties

The optical properties of **HQG1** and **HQG2** were investigated by UV-visible and photoluminescence (PL) spectroscopy in a dilute dichloromethane (CH_2Cl_2) solution as shown in **Figure 4.17, 4.18** and summarized in **Table 1**. UV-visible spectra of **HQG1** and **HQG2** exhibit two major absorption bands, an absorption band at 298 nm which could be assigned to the π - π^* local electron transition of the carbazole unit (Moonsin et al., 2012). The absorption band at 335 nm and 349 nm which could be assigned to the π - π^* local electron transition of the 8-hydroxyquinoline unit (Bardez et al., 1997). The molar absorptivity of **HQG2** was higher than **HQG1** because the G2-carbazole of **HQG2** has the number of carbazole more than G1-carbazole of **HQG1**, therefore **HQG2** has the value of molar absorptivity higher than **HQG1**. The onset absorption edge of **HQG1** and **HQG2** were 365 and 372 nm. The energy band gaps (E_g) of **HQG1** and **HQG2** were 3.40 and 3.33 eV, respectively. **HQG2** was slightly red-shifted when compared to **HQG1** because the energy band gap (E_g) of **HQG2** was lower than **HQG1**.

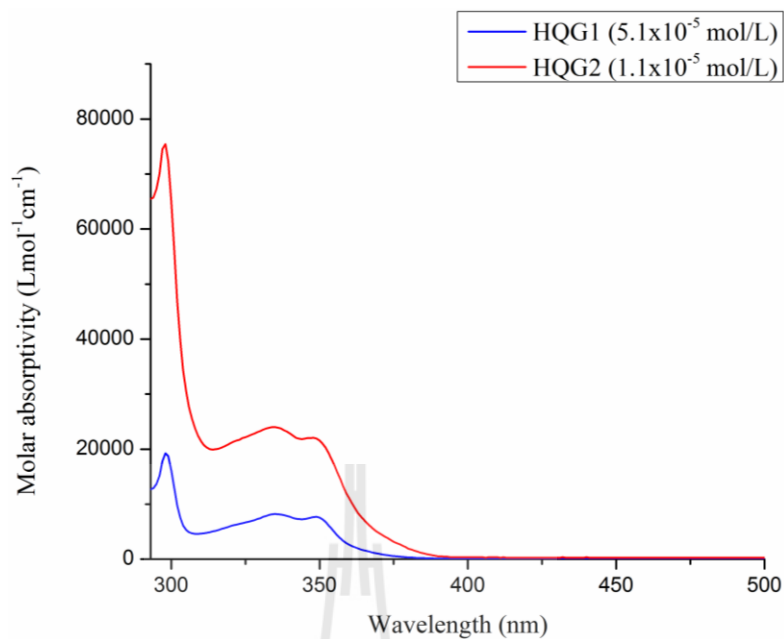


Figure 4.17 Absorption spectra of **HQG1** and **HQG2** in CH₂Cl₂.

Photoluminescence spectra of **HQG1** and **HQG2** are located in blue region with emission peaks at 372 nm and 402 nm as shown in **Figure 4.18**, respectively. The emission peak of **HQG2** was higher than **HQG1**, therefore **HQG2** was slightly red-shifted. Because the G2-carbazole of **HQG2** can donor more electron to phenoxide ring which increased the HOMO energy level when compared to G1-carbazole of **HQG1** in **Figure 4.19**.

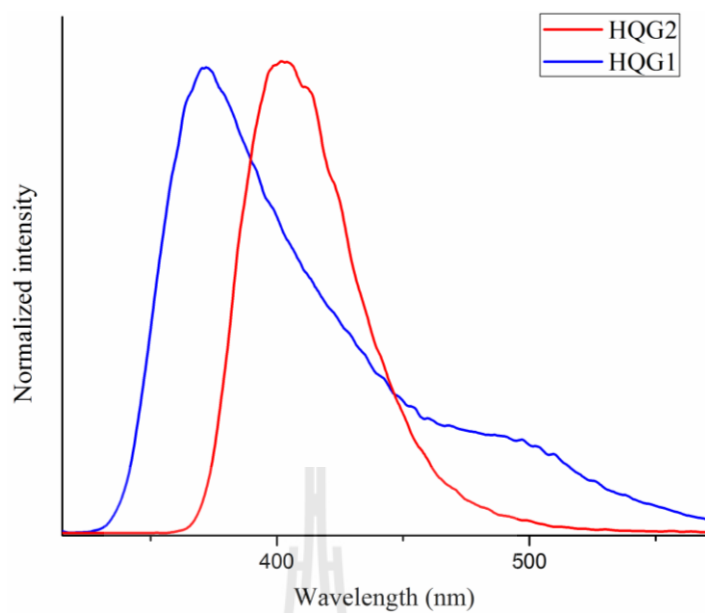


Figure 4.18 Fluorescence spectra of **HQG1** and **HQG2** in CH_2Cl_2 .

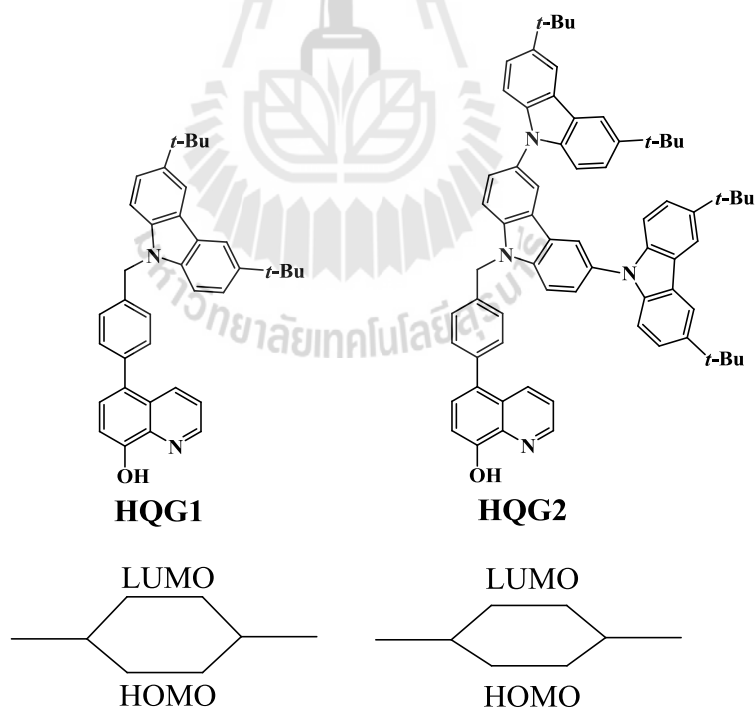


Figure 4.19 The energy levels of **HQG1** and **HQG2**.

Table 1.1 Summary of the physical data of **HQGn** (n = 1-2).

Compound	λ_{\max} of molar absorptivity (nm)	E_g (eV)	λ_{\max} of emission (nm)
HQG1	298, 335, 349	3.40	372
HQG2	298, 335, 349	3.33	402

4.3 Thermal properties

The thermal properties of **HQG1** and **HQG2** were determined by using differential scanning calorimetry (DSC) in nitrogen atmosphere at heating rate of 10 °C/min, the results are shown in **Figure 4.20**. DSC measurements of all compounds **HQG1** and **HQG2** showed the second order transition temperatures which had the glass transition temperatures (T_g) at 250.0 and 253.0 °C, respectively. The glass transition temperatures (T_g) of **HQG1** and **HQG2** were substantially higher than those of the commonly used HTMs which composed of **TPD** and **NPB**.

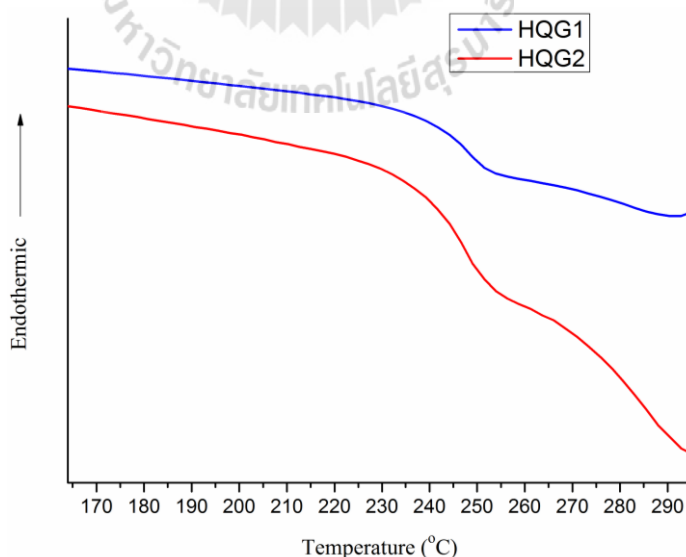


Figure 4.20 DSC traces of **HQG1** and **HQG2** measured under nitrogen atmosphere at heating rate of 10 °C/min.

The thermal stabilities of **HQG1** and **HQG2** were investigated by thermal gravimetric analyses (TGA) under nitrogen atmosphere at a heating rate of 10 °C/min. As shown in **Figure 4.33**, TGA measurement of **HQG1** exhibited high thermal decomposition temperature (T_d) at 416.1 °C, TGA measurement of **HQG2** showed high thermal decomposition temperature (T_d) at 508.0 °C.

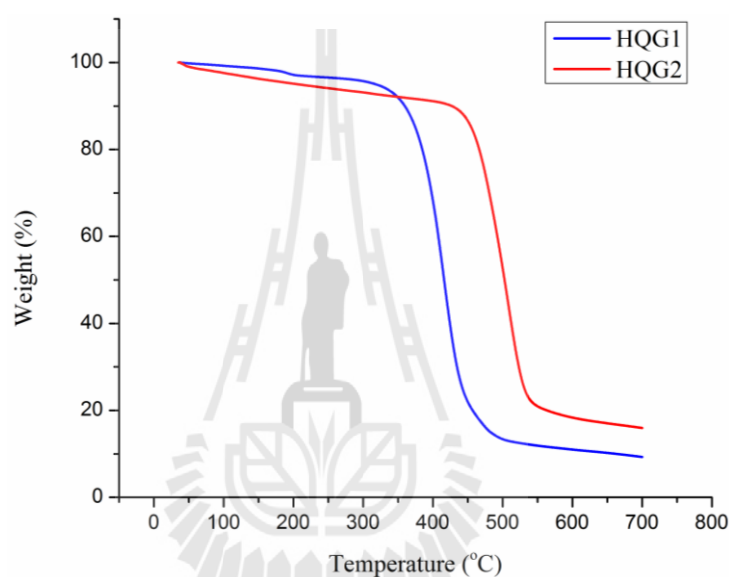


Figure 4.21 TGA of HQG1 and HQG2 measured under nitrogen atmosphere at heating rate of 10 °C/min.

Table 1.2 Thermal properties of **HQG_n** (n = 1-2).

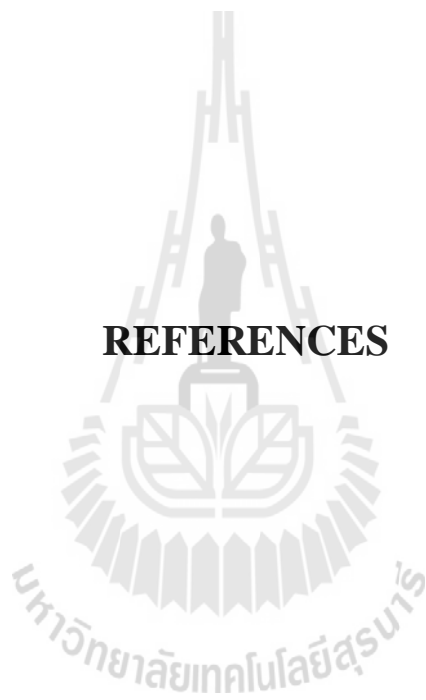
Compound	Temperature (°C)	
	T _g	T _d
HQG1	250.0	416.1
HQG2	253.0	508.0

CHAPTER V

CONCLUSIONS

In this thesis, the target molecules **HQG1** and **HQG2** were successfully synthesized and conveniently for use as hole-transporting materials in OLEDs. The UV-visible absorption of **HQG1** and **HQG2** can provide the band gap (E_g), which the band gaps of **HQG1** and **HQG2** were 3.40 and 3.33 eV. The photoluminescence can give the emission wavelength of **HQG1** and **HQG2** at 372 and 402 nm, respectively. **HQG2** showed red shifted when compared to **HQG1**. The newly synthesized **HQG1** and **HQG2** improved the thermal property when compared to the most commonly used hole transporting materials (HTMs), N,N'-diphenyl-N,N'-bis(1-naphthyl)-(1,1'-biphenyl)-4,4'-diamine (**NPB**) and N,N'-bis(3-methylphenyl)-N,N'-bis(phenyl)benzidine (**TPD**). TGA measurement reveals **HQG1** and **HQG2** which high thermal decomposition temperature (T_d) at 416.1 °C and 508.0 °C. Finally, the target molecules **HQG1** and **HQG2** were expected for use as good hole-transporting materials in organic light-emitting diodes.

REFERENCES



REFERENCES

- Agrawal, A.K. and Jenekhe, S.A. (1996). Electrochemical properties and electronic structures of conjugated polyquinolines polyanthrazolines. **Chemistry of Materials**. 8: 579-589.
- Ananth reddy, M., Thomas, A., Malleshm, G., Sridhar, B., Jayathirtha Rao, V. and Bhanuprakash, K. (2011). Synthesis of novel twisted carbazole–quinoxaline derivatives with 1,3,5-benzene core: bipolar molecules as hosts for phosphorescent OLEDs. **Tetrahedron Letters**. 52: 6942-6947.
- Bardez, E., Devol, I., Larrey, B. and Valeur, B. (1997). Excited-State Processes in 8-Hydroxyquinoline: Photoinduced Tautomerization and Solvation Effects. **Journal of chemical physics**. 101: 7786-7793.
- Bernanose, P. (1955). Organic electronic. **Journal of Chemical Physics**. 52: 509.
- Brinkmann, M., Gadret, G., Muccini, M., Taliani, C., Masciocchi, N. and Sironi, A. (2000). Correlation between molecular packing and optical properties in different crystalline polymorphs and amorphous thin films of mer-Tris(8-hydroxyquinoline)Aluminum(III). **Journal of the American Chemical Society**. 122: 5147-5157.
- Burroughes, J.H., Bradley D.D.C., Brown A.R., Marks R.N., MacKay K. and Friend R.H. (1990). Light-emitting diodes based on conjugated polymers. **Nature**. 347: 539-541.

- Chan, K.L., McKiernan M.J., Towns, C.R. and Holmes, A.B. (2005). Poly(2,7-dibenzosilole): A blue light emitting polymer. **Journal of the American Chemical Society**. 127: 7662-7663.
- Chan-Seok, O. and Jun-Yeob, L. (2014). High triplet energy Al complex as a host material for blue phosphorescent organic light-emitting diodes. **Organic Electronics**. 15: 1071-1075.
- Chen, J.P., Tanabe, H., Li, X.C., Thoms, T., Okamura, Y. and Ueno, K. (2003). Novel organic hole transport material with very high T_g for light-emitting diodes. **Synthetic Metals**. 132: 173-176.
- Chen, Z-K., Nancy, H.S.L, Wei, H., Xu Y-S. and Yong, C. (2003). Poly(arylenevinylene) and poly(heteroarylenevinylene) light emitting polymer and polymer light-emitting devices. **Macromolecules**. 36: 1009-1020.
- Deng, L., Li, J. and Li, W. (2014). Solution-processible small-molecular host materials for high-performance phosphorescent organic light-emitting diodes. **Dyes and Pigments**. 102: 150-158.
- Dresner, J. (1969). Double injection electroluminescence in anthracence. **RCA Review**. 30: 322-334.
- Fakhreldin, O., Saleh, N. and Khalifa, N. (2012). Synthesis characterization and DFT investigation of aluminum complexes of aryl-substituted-8-hydroxyquinoline. **Dyes and Pigments**. 92 : 1153-1159.
- Greenham, N.C., Moratti, S.C., Bradley, D.D.C., Friend, R.H. and Holmes, A.B. (1993). Efficient light-emitting-diodes based on polymers with high electron-affinities. **Nature**. 365: 628-630.

- Griniene, R., Grazulevicius, J.V., Tseng, K.Y., Wang, W.B., Jou, J.H. and Grazulevicius, S. (2011). Aryl substituted 9-(2,2-diphenylvinyl)carbazoles as efficient materials for hole transporting layers of OLEDs. **Synthetic Metals**. 161: 2466-2470.
- Gutmann, F., Lyons, L. and Keyzer, H. (1981). Organic Semiconductors. **Journal of Electronic Materials**. 20: 945-948 .
- Han, T.H., Lee, Y., Choi, M.R., Woo, S.H., Bae, S.H., Hong, B.H., Ahn, J.H. and Lee T.W. (2012). Extremely efficient flexible organic light-emitting diodes with modified graphene anode. **Nature Photonics**. 6: 105-110.
- Heiskanen, J.P. and Hormi, O.E.O. (2009). 4-Aryl-8-hydroxyquinolines from 4-chloro-8-tosyloxyquinoline using a Suzuki–Miyaura cross-coupling approach. **Tetrahedron**. 65: 518-524
- Hu, N., Xie, S., Popovic, Z., Ong, B. and Hor, A. (1999). 5,11-Dihydro-5,11-di-1-naphthylidolo[3,2-b]carbazole: atropisomerism in a novel hole-transport molecule for organic light-emitting diodes. **Journal of the American Chemical Society**. 121: 5097-5098.
- Huang, Q., Walzer, K., Pfeiffer, M., Lyssenko, V., He, G. and Leo, K. (2006). Handbook of Organic Materials for Optical and (Opto) Electronic Devices. **Applied Physics Letters**. 88: 113515.
- Ide, N., Tsuji, H., Ito, N., Sasaki, H., Nishimori, T. and Kuzuoka, Y. (2008). High-performance OLEDs and their application to lighting. **Proceedings of SPIE**. 7051: 705119-21.
- Kalinowski, J., (2005). Organic Light-Emitting Diodes Principle, Characteristics, and processes. **Marcel Dekker : New York**. 305: 253-266.

- Kallmann, H. and Pope, M. (1960). Organic Semiconductors. **Journal of Chemical Physics**. 32: 300.
- Kulkarni, A.P., Tonzola, C.J. Babel, A. and Jenekhe, S.A. (2004). Electron transport materials for organic light-emitting diodes. **Chemistry of Materials**. 16: 4556-4573.
- Li, J., Liu, D., Li, Y., Lee, C., Kwong, H. and Lee, S. (2000). A high T_g carbazole-based hole-transporting material for organic light-emitting devices. **Chemistry of Materials**. 17: 1208-1212.
- Moonsin, P., Prachumrak, N., Rattannawan, R., Keawin, T., Jungsuttiwong, S., Sudyoadsuk, T. and Promarak, V. (2012). Carbazole dendronised triphenylamines as solution processed high T_g amorphous hole-transporting materials for organic electroluminescent devices. **Chemical Communications**. 48: 3382-3384.
- Neef, C.J. and Ferraris, J.P. (2000). Organic light-emitting materials and devices. **Macromolecules**. 33: 2311-2314.
- Partridge, R. (1983). Synthesis and properties of a novel brush-type copolymer bearing thiophene backbone and 3-(N-carbazolyl)propyl acrylate side chains for light emitting applications. **Polymer**. 24: 733.
- Pope, M., Ilmann, H.P. and Magnante, P. (1963). Electroluminescence in Organic Crystals. **Journal of Chemical Physics**. 38: 2042.
- Pope, M. and Swenberg, C.E. (1999). Electronic Processes in Organic Crystals and Polymers. **Oxford University**.

- Pudzich, R., Fuhrmann-Lieker, T. and Salbeck, J. (2006). Spiro compounds for organic electroluminescence and related applications. **Emissive Materials: Nanomaterials**. 199: 83-142.
- Qian, Y., Cao, F. and Guo, W. (2013). High thermal stability 3, 6-fluorene-carbazole-dendrimers as host materials for efficient solution-processed blue phosphorescent devices. **Tetrahedron**. 69: 4163-4175.
- Rajagopal, A., Wu, C.I. and Kahn, A. (1998). Energy level offset at organic semiconductor heterojunctions. **Journal of Applied Physics**. 83: 2649-2655.
- Robert, E., Wrigley, T.I. and Young, W.G. (1958). The reaction of thionyl chloride with steroid allylic alcohols. **Journal of the American Chemical Society**. 80: 4604-4606.
- Rothmann, M.M., Fuchs, E., Schildknecht, C., Langer, N, Lennartz, C, Munstar, I. and Strohriegl, P. (2011). Designing a bipolar host material for blue phosphorescent OLEDs: Phenoxy-carbazole substituted triazine. **Organic Electronics**. 12: 1192-1197.
- Sano, T., Fujita, M., Fujii, T., Hamada, Y., Shibata, K. and Kuroki, K. (1995). Novel europium complex for electroluminescent devices with sharp red emission. **Journal of Applied Physics**. 34: 1883.
- Schwartz, G., Reineke, S., Rosenow, T.C., Walzer, K. and Leo, K. (2009). Densely packed arrays of ultra-high-aspect-ratio silicon nanowires fabricated using block copolymer lithography and metal-assisted etching. **Advanced Functional Materials**. 19: 1.
- Schwoerer, M. and Wolf, H.C. (2007). Molecular designs toward improving organic photovoltaics. **Organic Molecular Solid**. 91: 243502.

- Segura, J.L. (1998). The chemistry of electroluminescent organic materials. **Actapolymerica**. 49: 319.
- Seung, W.K., Byung, J.J., Taek, A. and Hong, K.S. (2002). Light emitting layers for LED devices based on high T_g polymer matrix compositions. **Macromolecules**. 35: 6217-6223.
- Singh, G., Bhalla, V. and Kumar, M. (2015). Carbazole end-capped and triphenylamine-centered starburst derivative for hole-transport in electroluminescent devices. **Optical Materials**. 46: 82-87.
- Szu-Hung, L., Jin-Ruei, S., Shun-Wei, L., Shi-Jay, Y., Yu-Hung, C. and Chih-I, W. (2008). The hydroxynaphthyridine-Derived Group III Metal Chelates: Wide B and Gap and Deep Blue Analogues of Green Alq3 (Tris(8-hydroxyquinolate)aluminum) and Their Versatile Applications for Organic Light-Emitting Diodes. **Journal of the American Chemical Society**. 131: 763-777.
- Tandon, K., Ramasesha, S. and Mazumdar, S. (2003). Electron correlation effects in electron-hole recombination in organic light-emitting diodes. **Physical Review B**. 67: 045109.
- Tang, C.W. and Vanslyke, S.A. (1987). Organic electroluminescent diodes. **Applied Physics Letters**. 51: 91-915.
- Thejokalyani, N. and Dhoble, S.J. (2012). High efficiency solution processed fluorescent yellow organic light-emitting diode through fluorinated alcohol treatment at the emissive layer/cathode interface. **Renewable Sustainable Energy Reviews**. 16: 2696-2723.

- Wang, X., Feng, L. and Chen, Z. (2008). Synthesis and photophysics of novel 8-hydroxyquinoline aluminum metal dye with hole transfer groups. **Spectrochimica Acta Part A**. 71: 1433-1437
- Wohlgemant, M., Tandon, K., Mazumdar, S., Ramasesha, S. and Vardeny, Z.V. (2001). Formation cross-sections of singlet and triplet excitons in pi-conjugated polymers. **Nature**. 409: 494-497.
- Wu, C., Silu, T., Chen, M., Mo, H., Liu, X., Zhang, X., Zhao, W. and Lee C.H. (2013). A new multifunctional fluorenyl carbazole hybrid for high performance deep blue fluorescence, orange phosphorescent host and fluorescence/phosphorescence white OLEDs. **Dyes and Pigments**. 97: 273-277.
- Wyckhoff, R. (1963). Crystal structure descriptions. **New York : Wiley**. 1: 28.
- Yang, W., Chen, Y., Jiang, W., Ban, X., Huang, B., Dai, Y. and San, Y. (2013). A carbazole-based dendritic host material for efficient solution processed blue phosphorescent OLEDs. **Dyes and Pigments**. 97: 286-290.
- Yue, Y. (2004). Experimental evidence for the existence of an ordered structure in a silicate liquid above its liquidus temperature. **Journal of Non-Crystalline Solids**. 345: 523-527.
- Zhang, T., Liu, D., Wang, Y., Bao, S. and Zhang, S. (2015). Novel carbazole dendronized oligofluorenes for solution-processed organic light-emitting diodes. **Dyes and Pigments**. 122: 295-301.

APPENDICES

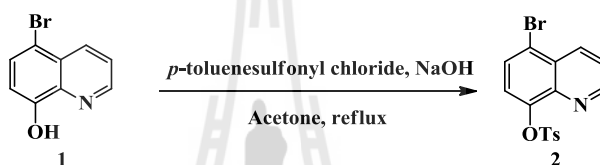


APPENDIX A

CALCULATION % YIELD

A.1 Calculation % yield

A.1.1 Calculation % yield of **compound 2**



Calculation of weight (g) of **compound 2** in theory

1 mole of **compound 1** = 1 mole of **compound 2**

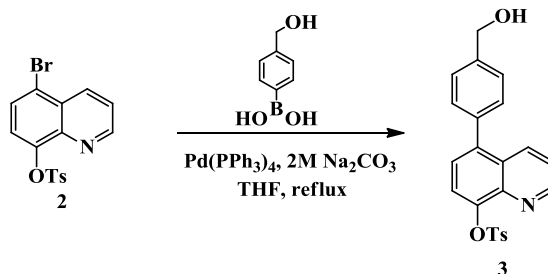
$$\frac{\text{g of compound 1}}{\text{MW of compound 1}} = \frac{\text{g of compound 2}}{\text{MW of compound 2}}$$

$$\text{g of compound 2} = \frac{\text{g of compound 1}}{\text{MW of compound 1}} \times \text{MW of compound 2}$$

$$\text{g of compound 2} = \frac{5.00 \text{ g} \times 378.24}{224.05} = 8.44 \text{ g}$$

$$\% \text{ yield} = \frac{\text{g of compound 2}}{\text{g of compound 2 in theory}} \times 100 = \frac{7.99 \text{ g}}{8.44 \text{ g}} \times 100 = 95\%$$

A.1.2 Calculation % yield of **compound 3**



Calculation of weight (g) of **compound 3** in theory

1 mole of **compound 2** = 1 mole of **compound 3**

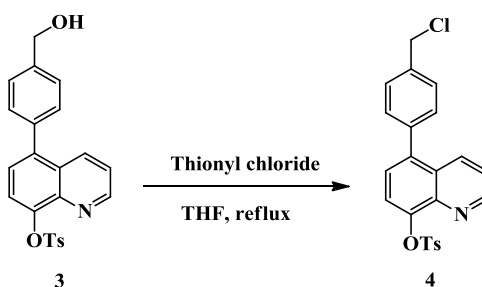
$$\frac{\text{g of compound 2}}{\text{MW of compound 2}} = \frac{\text{g of compound 3}}{\text{MW of compound 3}}$$

$$\text{g of compound 3} = \frac{\text{g of compound 2}}{\text{MW of compound 2}} \times \text{MW of compound 3}$$

$$\text{g of compound 3} = \frac{2.00 \text{ g} \times 405.47}{378.24} = 2.14 \text{ g}$$

$$\% \text{ yield} = \frac{\text{g of compound 3}}{\text{g of compound 3 in theory}} \times 100 = \frac{1.92 \text{ g}}{2.14 \text{ g}} \times 100 = 90\%$$

A.1.3 Calculation % yield of **compound 4**



Calculation of weight (g) of **compound 4** in theory

1 mole of **compound 3** = 1 mole of **compound 4**

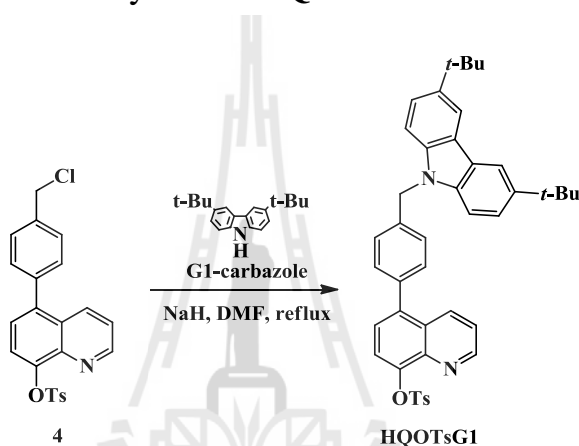
$$\frac{\text{g of compound 3}}{\text{MW of compound 3}} = \frac{\text{g of compound 4}}{\text{MW of compound 4}}$$

$$\text{g of compound 4} = \frac{\text{g of compound 3}}{\text{MW of compound 3}} \times \text{MW of compound 4}$$

$$\text{g of compound 4} = \frac{1.92 \text{ g} \times 423.91}{405.47} = 2.01 \text{ g}$$

$$\% \text{ yield} = \frac{\text{g of compound 4}}{\text{g of compound 4 in theory}} \times 100 = \frac{1.94 \text{ g}}{2.01 \text{ g}} \times 100 = 97\%$$

A.1.4 Calculation % yield of HQOTsG1



Calculation of weight (g) of HQOTsG1 in theory

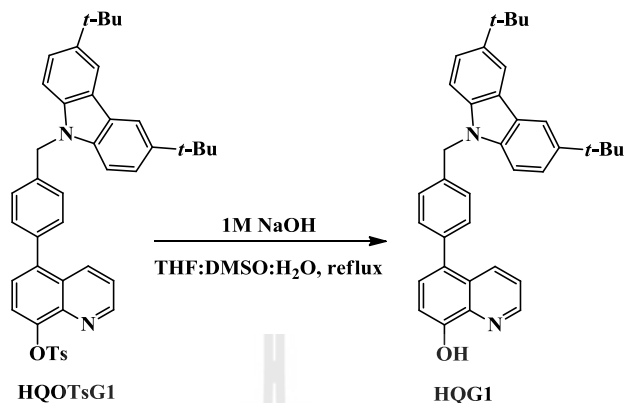
1 mole of compound 4 = 1 mole of HQOTsG1

$$\frac{\text{g of compound 4}}{\text{MW of compound 4}} = \frac{\text{g of HQOTsG1}}{\text{MW of HQOTsG1}}$$

$$\text{g of HQOTsG1} = \frac{\text{g of compound 4}}{\text{MW of compound 4}} \times \text{MW of HQOTsG1}$$

$$\text{g of HQOTsG1} = \frac{0.50 \text{ g} \times 666.87}{423.91} = 0.79 \text{ g}$$

$$\% \text{ yield} = \frac{\text{g of HQOTsG1}}{\text{g of HQOTsG1 in theory}} \times 100 = \frac{0.70 \text{ g}}{0.79 \text{ g}} \times 100 = 89\%$$

A.1.5 Calculation % yield of **HQG1**

Calculation of weight (g) of **HQG1** in theory

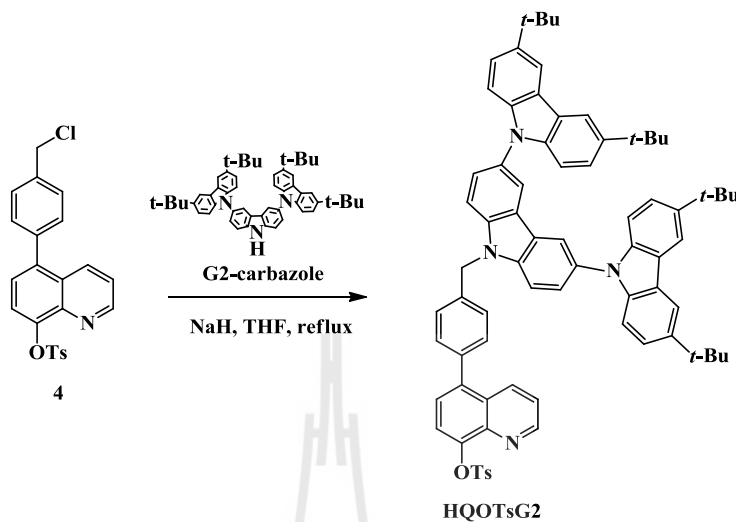
1 mole of **HQOTsG1** = 1 mole of **HQG1**

$$\frac{\text{g of HQOTsG1}}{\text{MW of HQOTsG1}} = \frac{\text{g of HQG1}}{\text{MW of HQG1}}$$

$$\text{g of HQG1} = \frac{\text{g of HQOTsG1}}{\text{MW of HQOTsG1}} \times \text{MW of HQG1}$$

$$\text{g of HQG1} = \frac{0.70 \text{ g} \times 512.68}{666.87} = 0.54 \text{ g}$$

$$\% \text{ yield} = \frac{\text{g of HQG1}}{\text{g of HQG1 in theory}} \times 100 = \frac{0.53 \text{ g}}{0.54 \text{ g}} \times 100 = 98\%$$

A.1.6 Calculation % yield of **HQOTsG2**

Calculation of weight (g) of **HQOTsG2** in theory

1 mole of **compound 4** = 1 mole of **HQOTsG2**

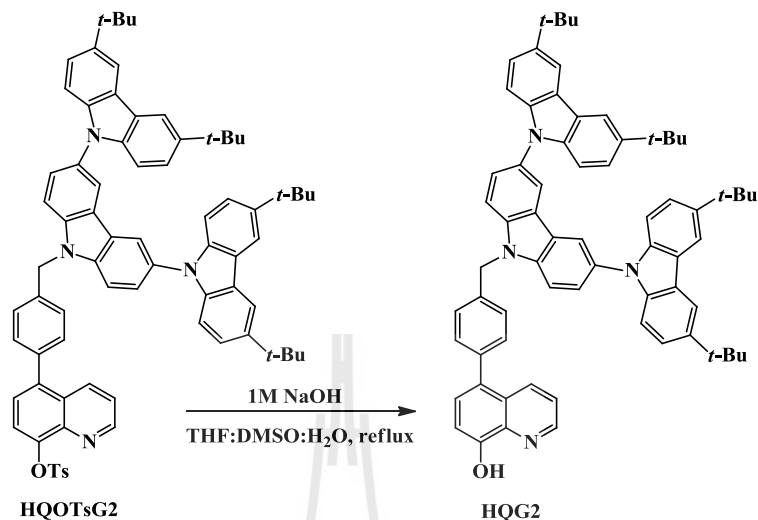
$$\frac{\text{g of compound 4}}{\text{MW of compound 4}} = \frac{\text{g of HQOTsG2}}{\text{MW of HQOTsG2}}$$

$$\text{g of HQOTsG2} = \frac{\text{g of compound 4}}{\text{MW of compound 4}} \times \text{MW of HQOTsG2}$$

$$\text{g of HQOTsG2} = \frac{0.50 \text{ g} \times 1109.46}{423.91} = 1.31 \text{ g}$$

$$\% \text{ yield} = \frac{\text{g of HQOTsG2}}{\text{g of HQOTsG2 in theory}} \times 100 = \frac{1.11 \text{ g}}{1.31 \text{ g}} \times 100 = 85\%$$

A.1.7 Calculation % yield of **HQG2**



Calculation of weight (g) of **HQG2** in theory

1 mole of **HQOTsG2** = 1 mole of **HQG2**

$$\frac{\text{g of HQOTsG2}}{\text{MW of HQOTsG2}} = \frac{\text{g of HQG2}}{\text{MW of HQG2}}$$

$$\text{g of HQG2} = \frac{\text{g of HQOTsG2}}{\text{MW of HQOTsG2}} \times \text{MW of HQG2}$$

$$\text{g of HQG2} = \frac{1.11 \text{ g} \times 955.28}{1109.46} = 0.96 \text{ g}$$

$$\% \text{ yield} = \frac{\text{g of HQG2}}{\text{g of HQG2 in theory}} \times 100 = \frac{0.94 \text{ g}}{0.96 \text{ g}} \times 100 = 98\%$$

A.2 Calculation energy band gap (E_g)

A.2.1 Calculation energy band gap (E_g) of **HQG1** ($\lambda_{\text{onset}} = 363 \text{ nm}$)

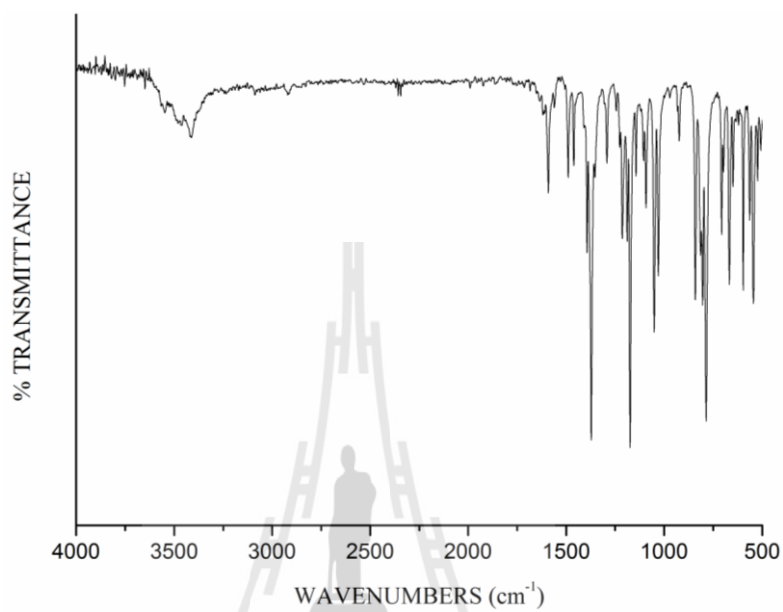
$$E_g \text{ (eV)} = 1240/\lambda_{\text{onset}} = 1240/365 = 3.40 \text{ eV}$$

A.2.2 Calculation energy band gap (E_g) of **HQG2** ($\lambda_{\text{onset}} = 371 \text{ nm}$)

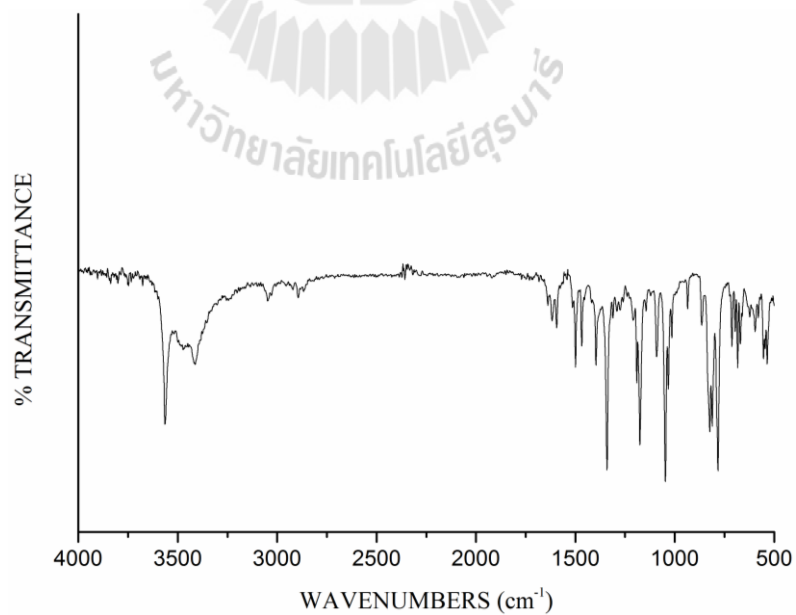
$$E_g \text{ (eV)} = 1240/\lambda_{\text{onset}} = 1240/372 = 3.33 \text{ eV}$$

A.3 IR-spectrum

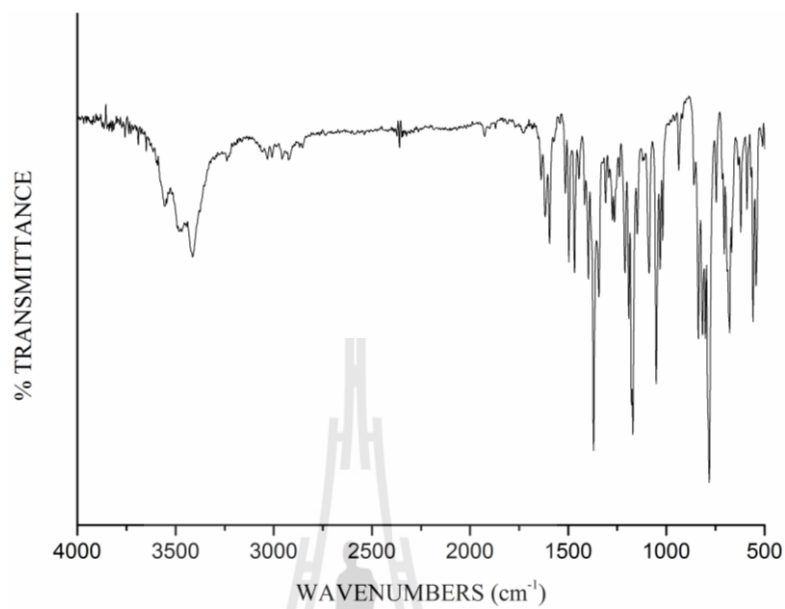
A.3.1 Compound 2



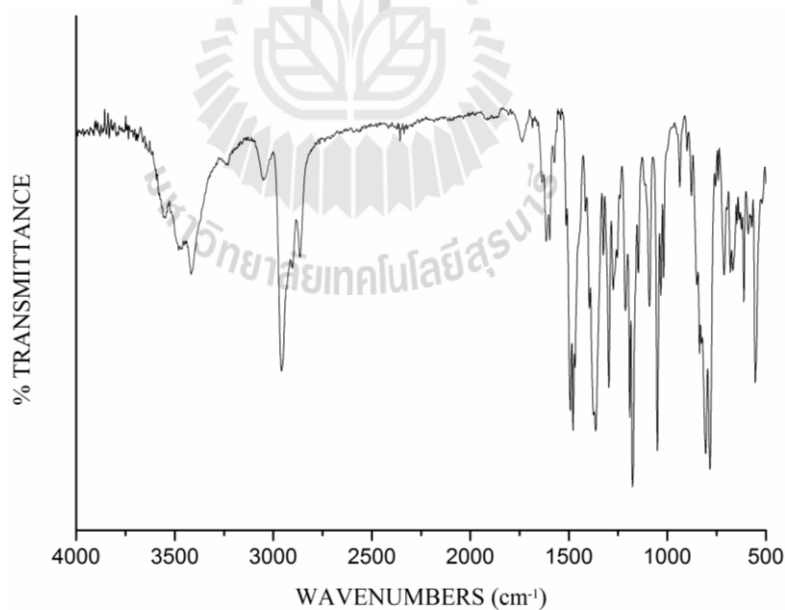
A.3.2 Compound 3



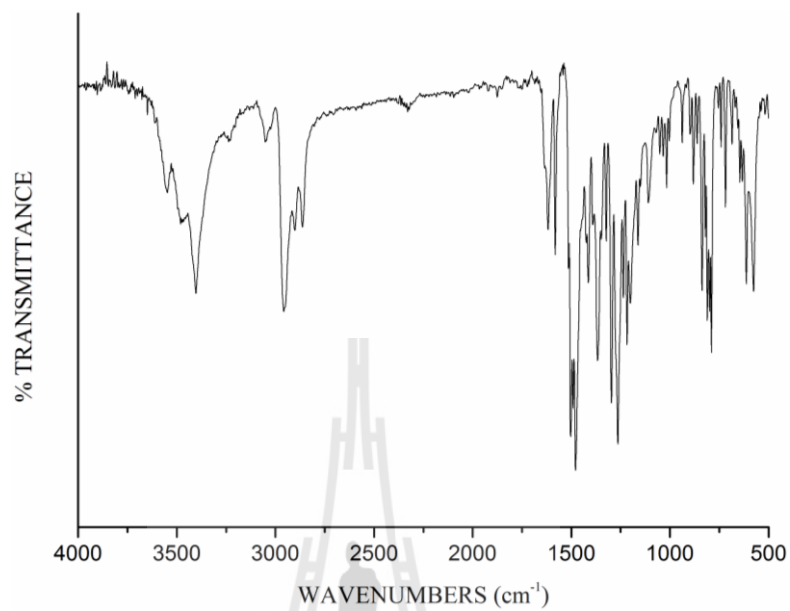
A.3.3 Compound 4



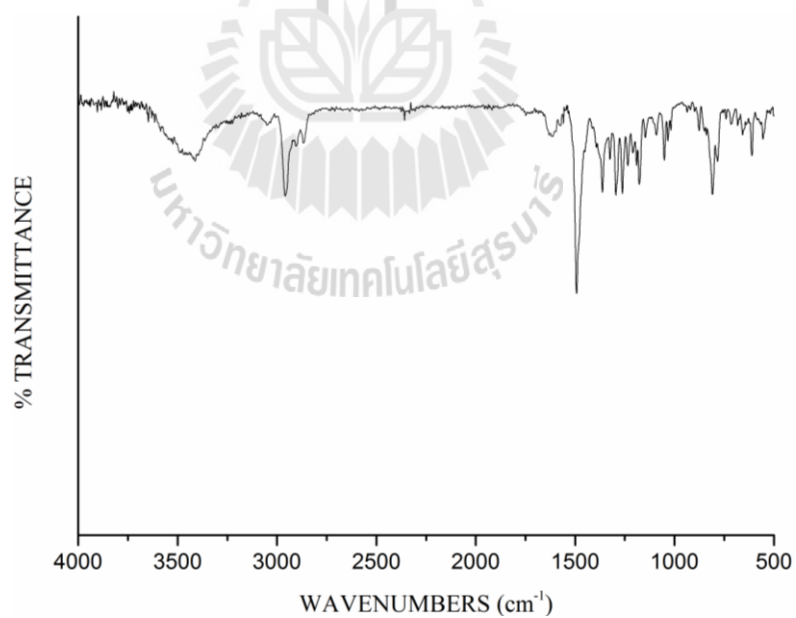
A.3.4 HQOTsG1



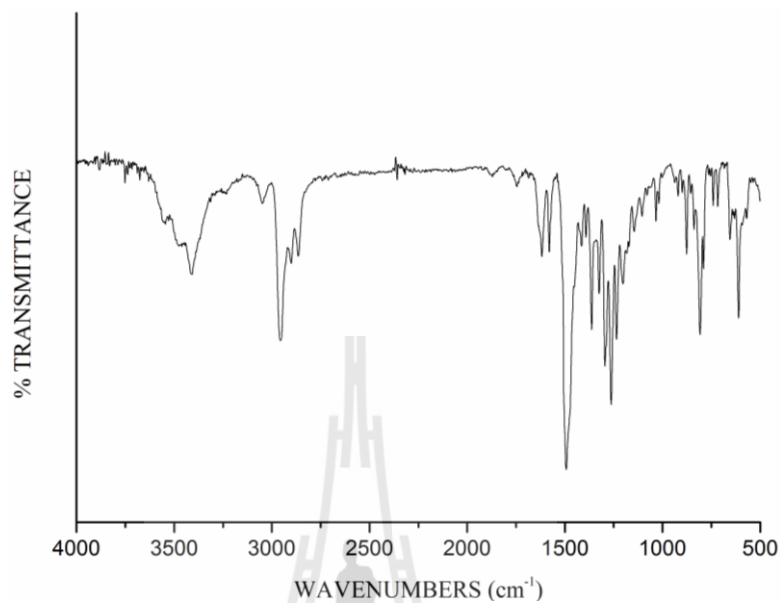
A.3.5 HQG1



A.3.6 HQOTsG2

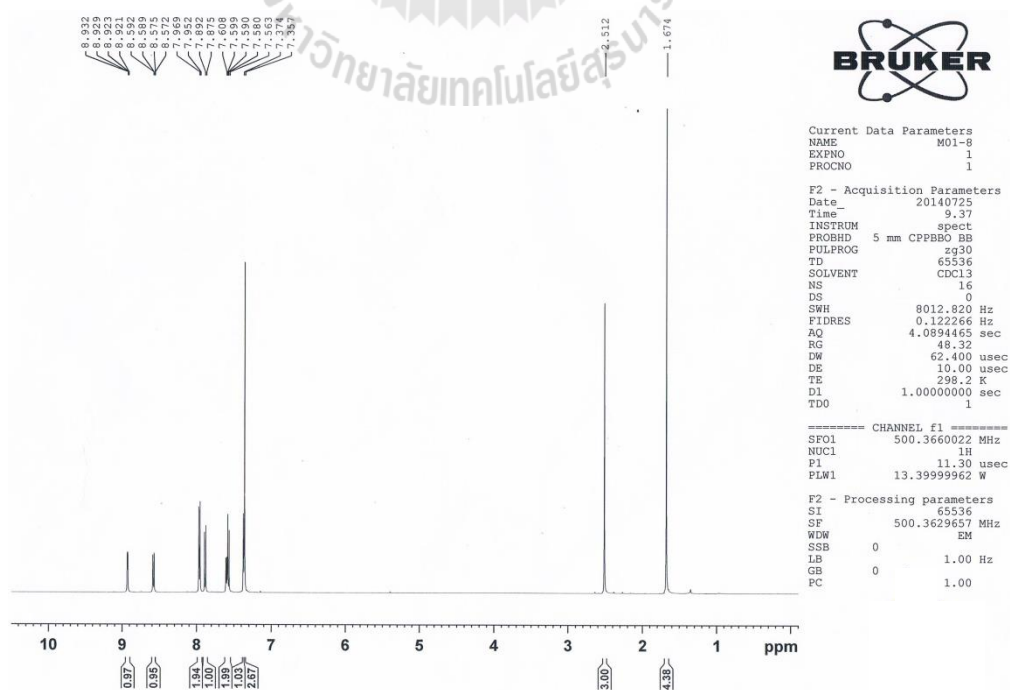


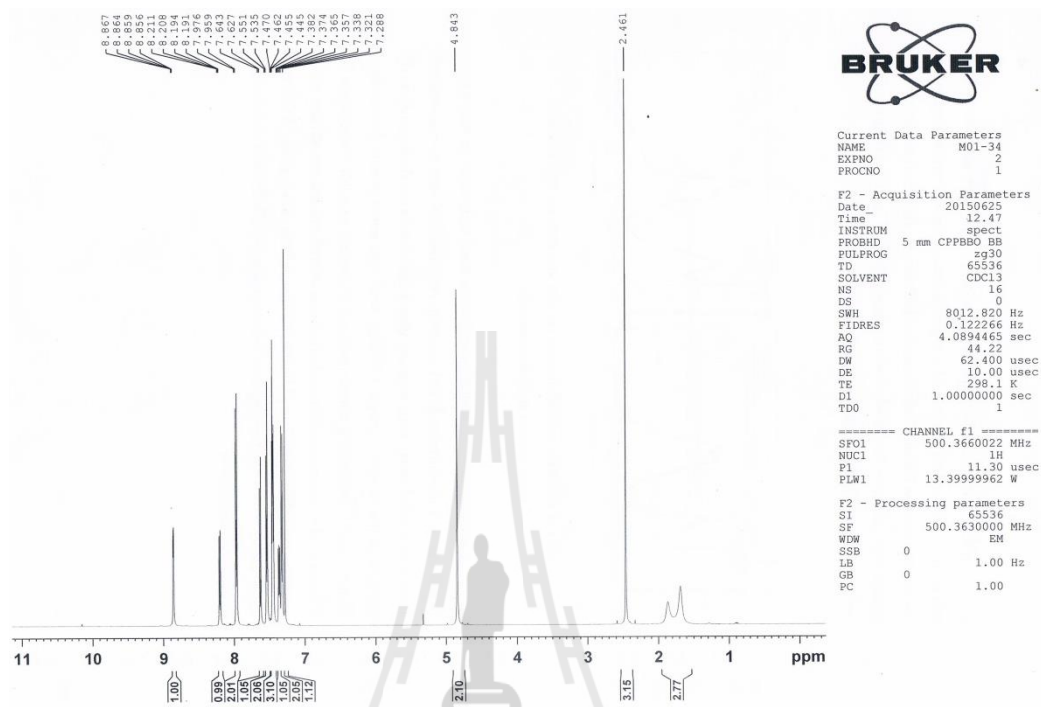
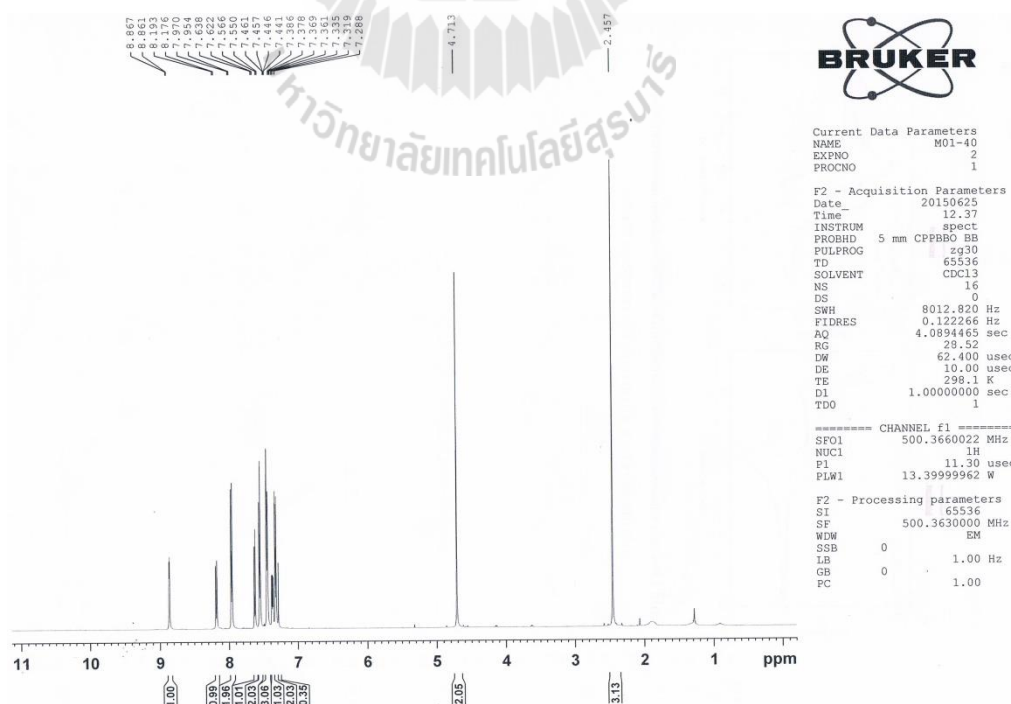
A.3.7 HQG2

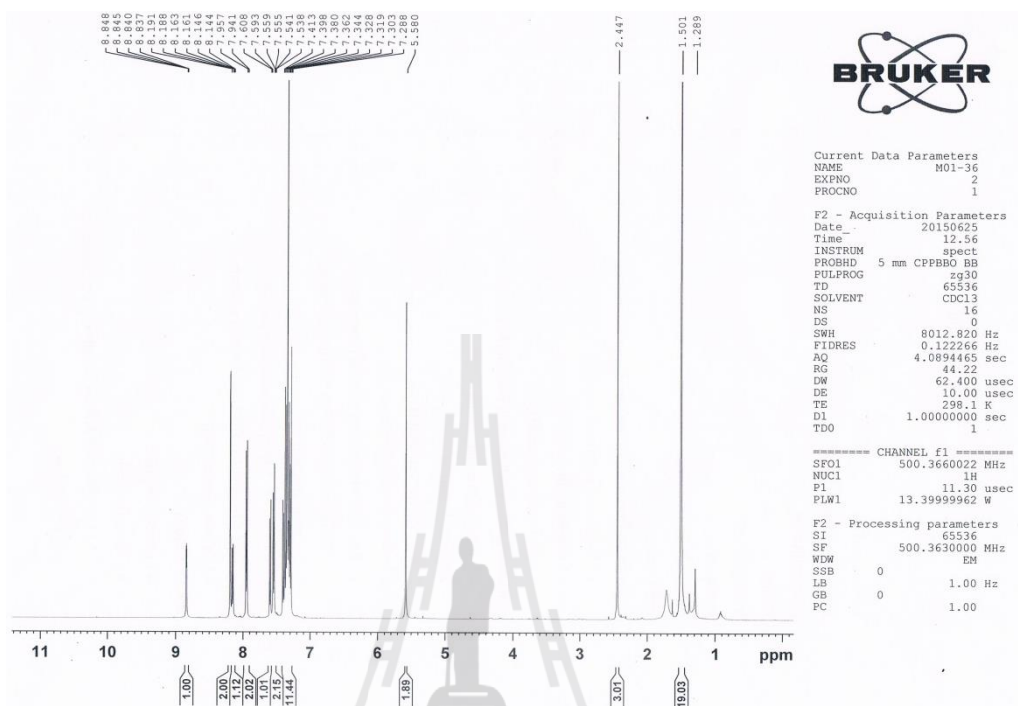
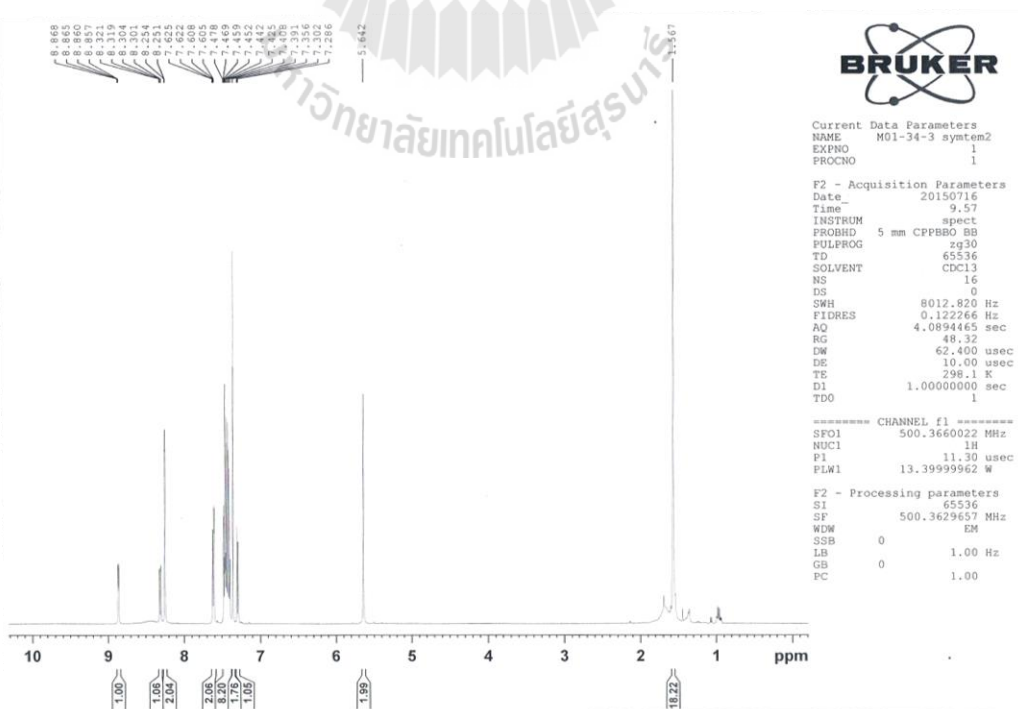


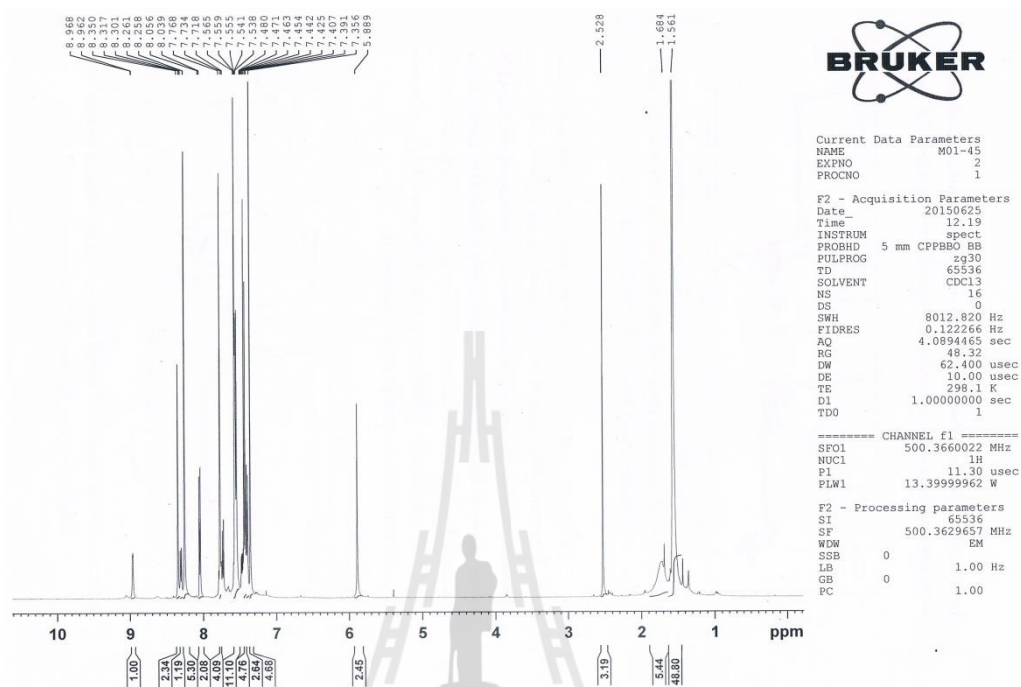
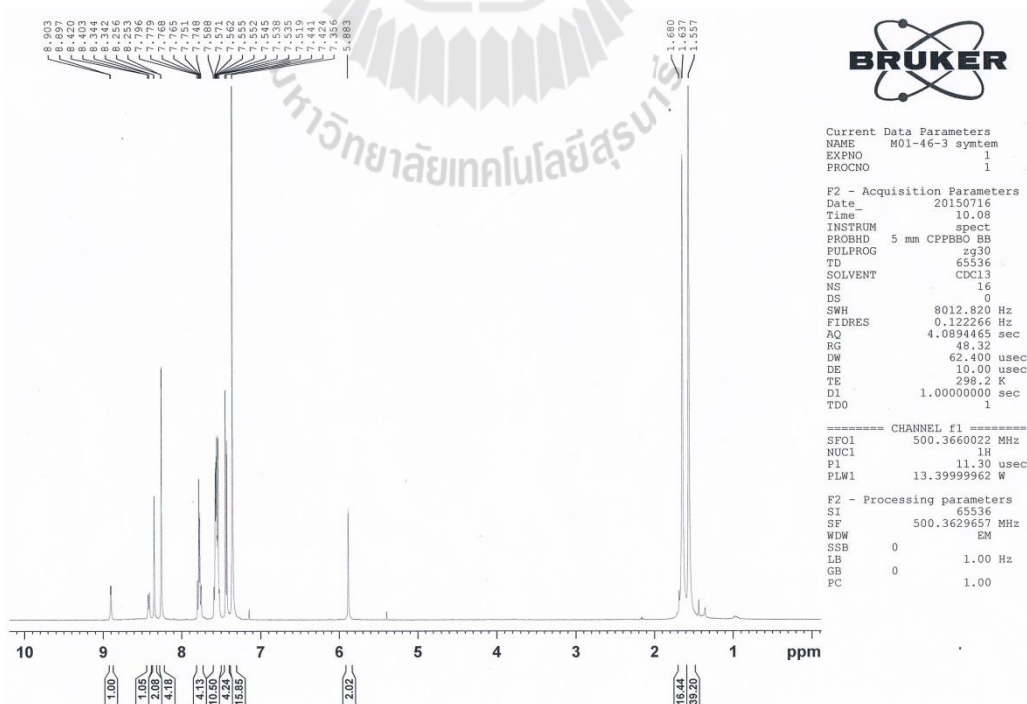
A.4 ¹H-NMR spectrum

A.4.1 ¹H-NMR spectrum of compound 2



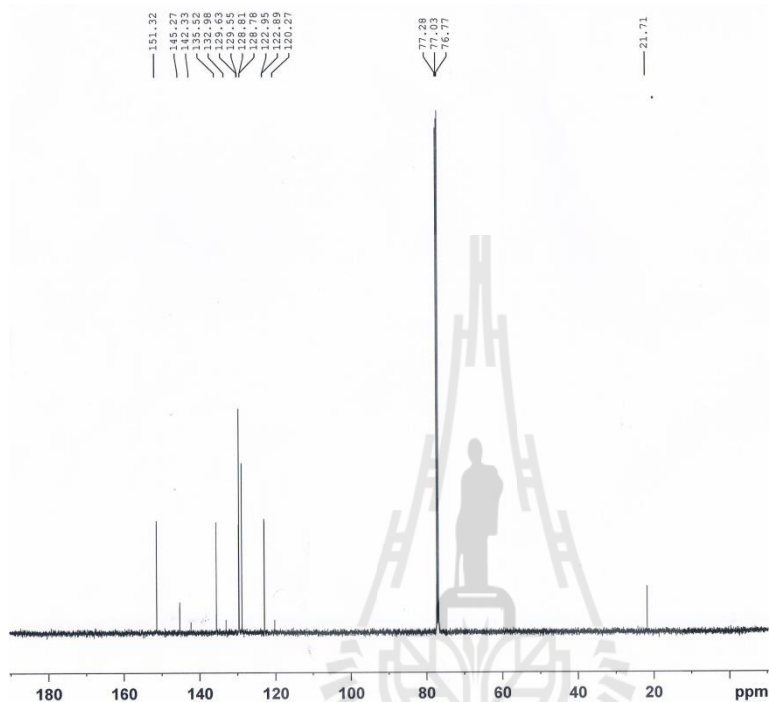
A.4.2 $^1\text{H-NMR}$ spectrum of compound 3A.4.3 $^1\text{H-NMR}$ spectrum of compound 4

A.4.4 ^1H -NMR spectrum of HQOTsG1A.4.5 ^1H -NMR spectrum of HQG1

A.4.6 $^1\text{H-NMR}$ spectrum of HQOTsG2A.4.7 $^1\text{H-NMR}$ spectrum of HQG2

A.5 ^{13}C -NMR spectrum

A.5.1 ^{13}C -NMR spectrum of compound 2



```

Current Data Parameters
NAME          M01-8
EXPNO         2
PROCNO        1

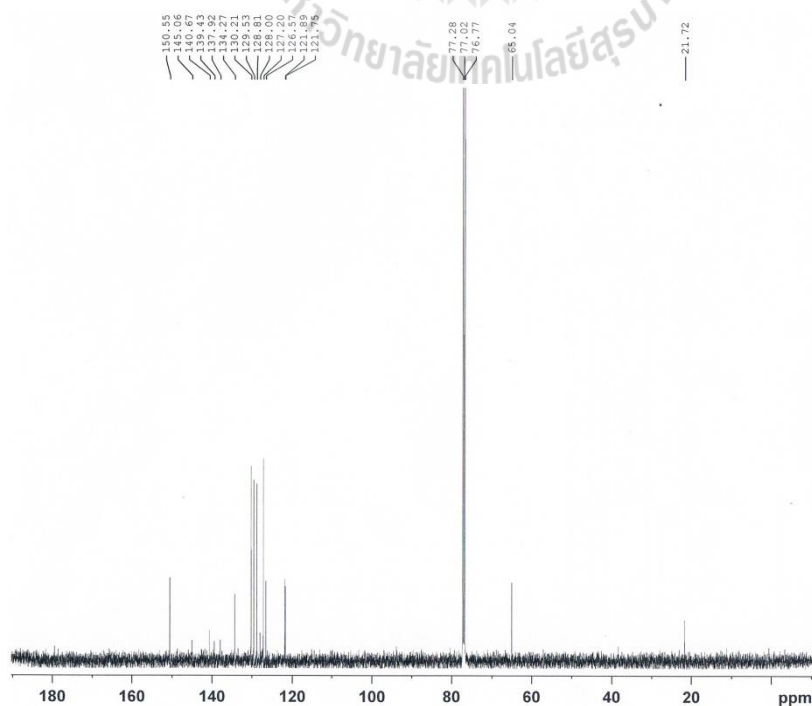
F2 - Acquisition Parameters
Date_         20140725
Time          9.55
INSTRUM       spect
PROBHD        5 mm CPPBBO BB
PULPROG       zgdc
TD            65536
SOLVENT       CDC13
NS            256
DS            4
SWH           25252.525 Hz
FIDRES        0.385323 Hz
AQ            1.2976128 sec
RG            195.01
DW            19.800 usec
DE            18.00 usec
TE            298.2 K
D1            1.5000000 sec
D11           0.0300000 sec
TDO           1

===== CHANNEL f1 =====
SFO1          125.8276995 MHz
NUC1          13C
P1            9.00 usec
PLW1          69.00000000 W

===== CHANNEL f2 =====
SFO2          500.3650015 MHz
NUC2          1H
CPDPRG2       waltz16
PCPD2         80.00 usec
PLW2          13.39999962 W
PLW12         0.26734999 W

F2 - Processing parameters
SI            32768
SF            125.8163760 MHz
WDW           EM
SSB           0
LB            1.00 Hz
GB            0
PC            1.40
  
```

A.5.2 ^{13}C -NMR spectrum of compound 3



```

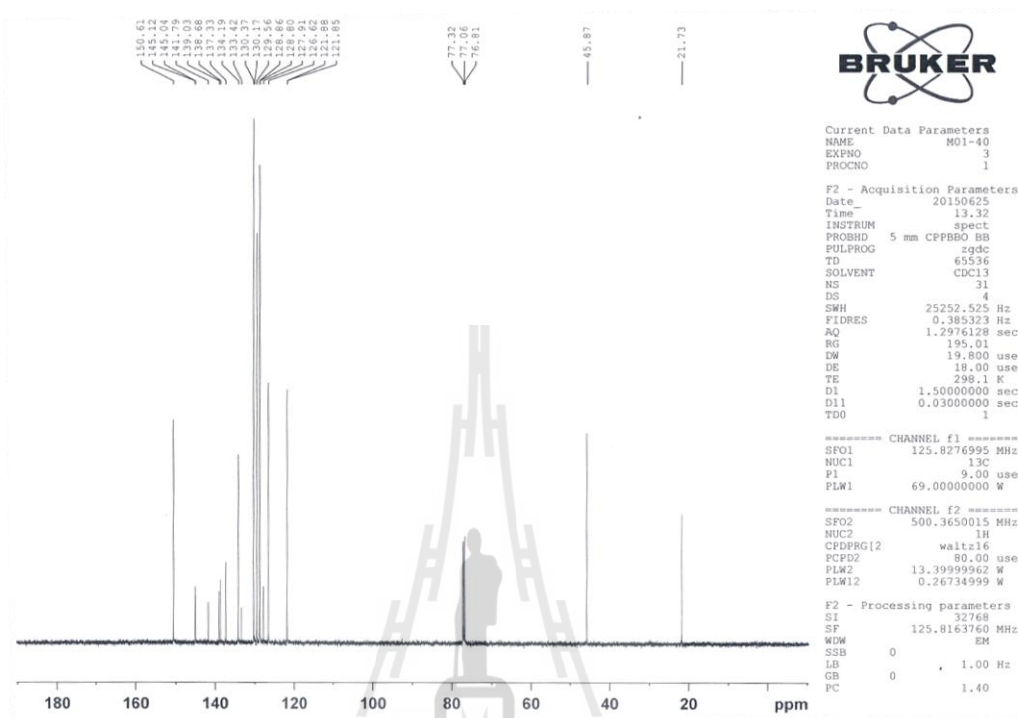
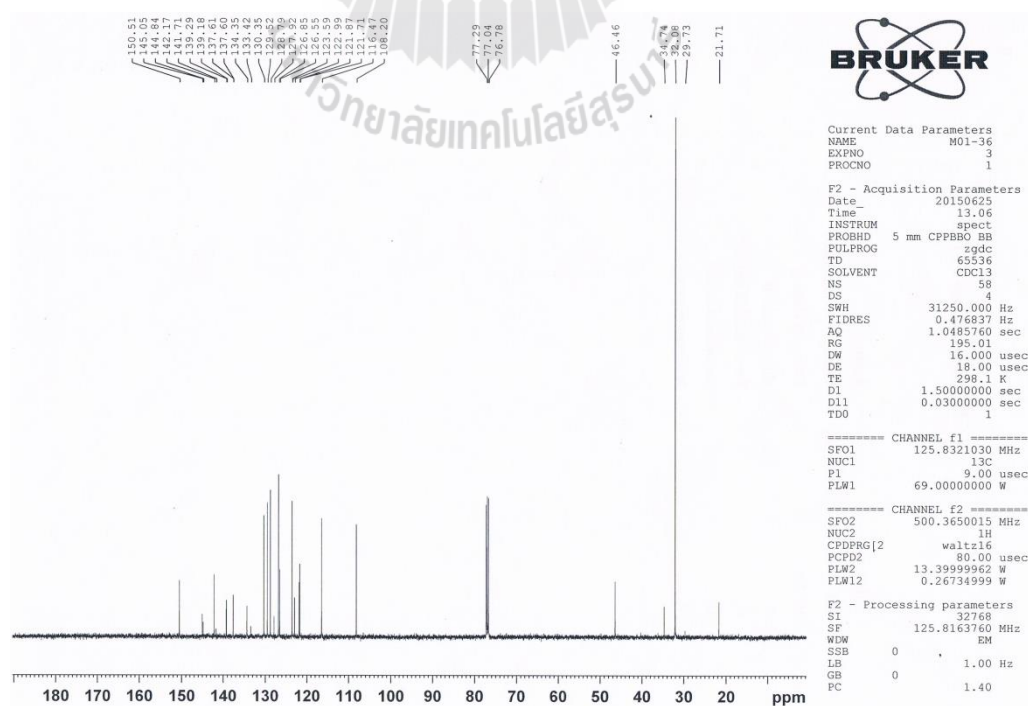
Current Data Parameters
NAME          M01-34-2
EXPNO         2
PROCNO        1

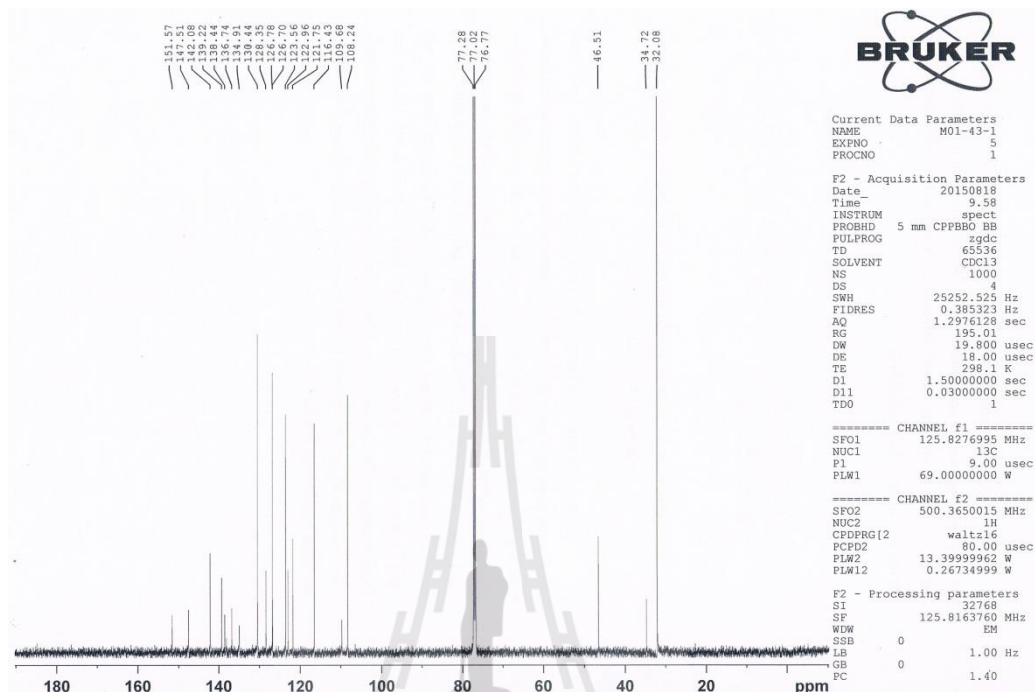
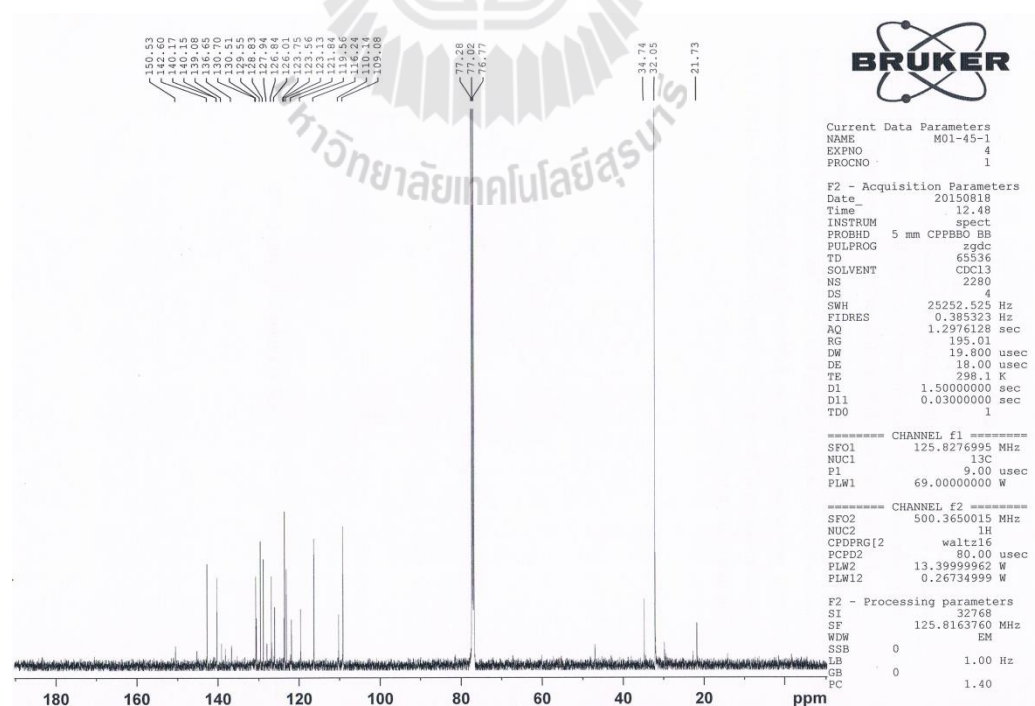
F2 - Acquisition Parameters
Date_         20150716
Time          9.41
INSTRUM       spect
PROBHD        5 mm CPPBBO BB
PULPROG       zgdc
TD            65536
SOLVENT       CDC13
NS            256
DS            4
SWH           25252.525 Hz
FIDRES        0.385323 Hz
AQ            1.2976128 sec
RG            195.01
DW            19.800 usec
DE            18.00 usec
TE            298.1 K
D1            1.5000000 sec
D11           0.0300000 sec
TDO           1

===== CHANNEL f1 =====
SFO1          125.8276995 MHz
NUC1          13C
P1            9.00 usec
PLW1          69.00000000 W

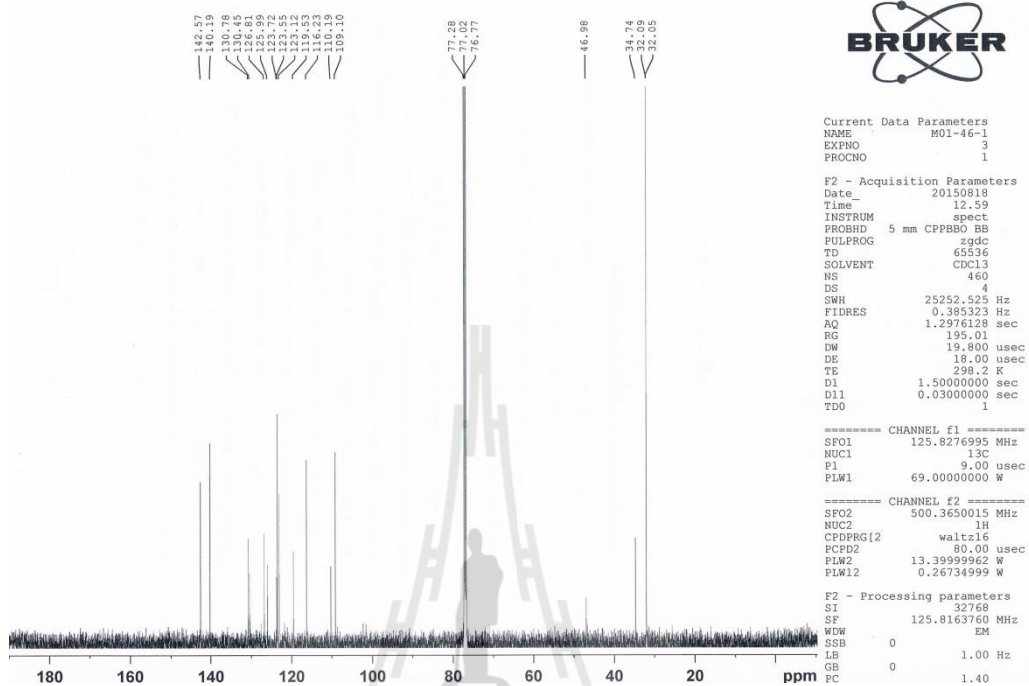
===== CHANNEL f2 =====
SFO2          500.3650015 MHz
NUC2          1H
CPDPRG2       waltz16
PCPD2         80.00 usec
PLW2          13.39999962 W
PLW12         0.26734999 W

F2 - Processing parameters
SI            32768
SF            125.8163760 MHz
WDW           EM
SSB           0
LB            1.00 Hz
GB            0
PC            1.40
  
```

A.5.3 ^{13}C -NMR spectrum of compound 4A.5.4 ^{13}C -NMR spectrum of HQOTsG1

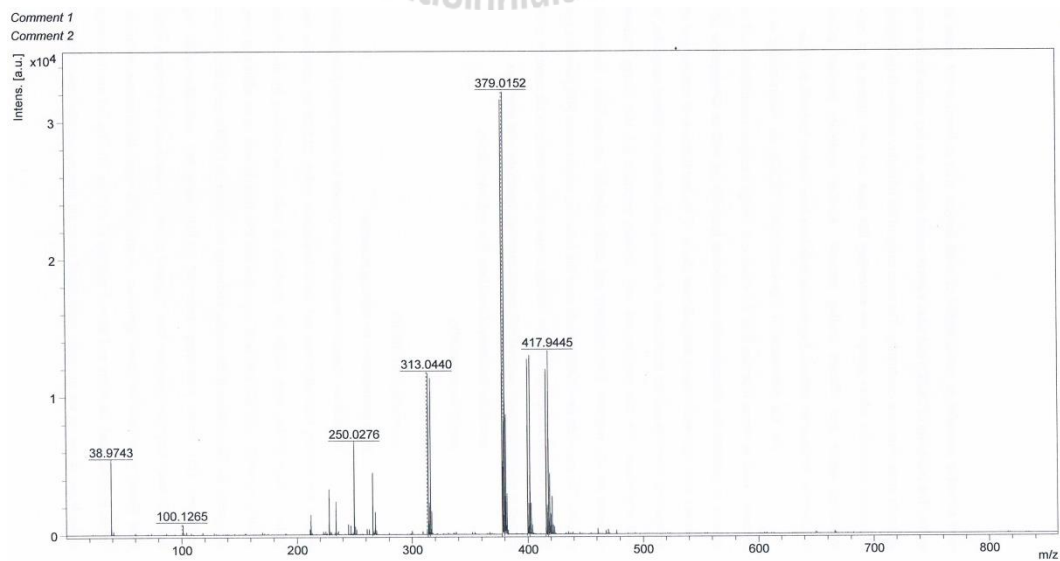
A.5.5 ^{13}C -NMR spectrum of HQG1A.5.6 ^{13}C -NMR spectrum of HQOTsG2

A.5.7 ^{13}C -NMR spectrum of HQG2

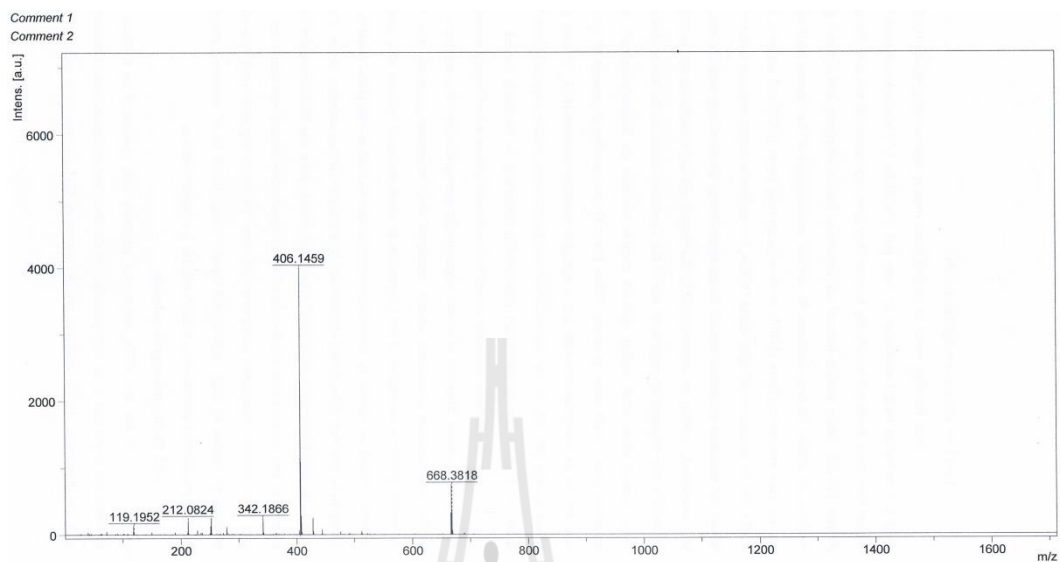


A.6 Mass spectrum

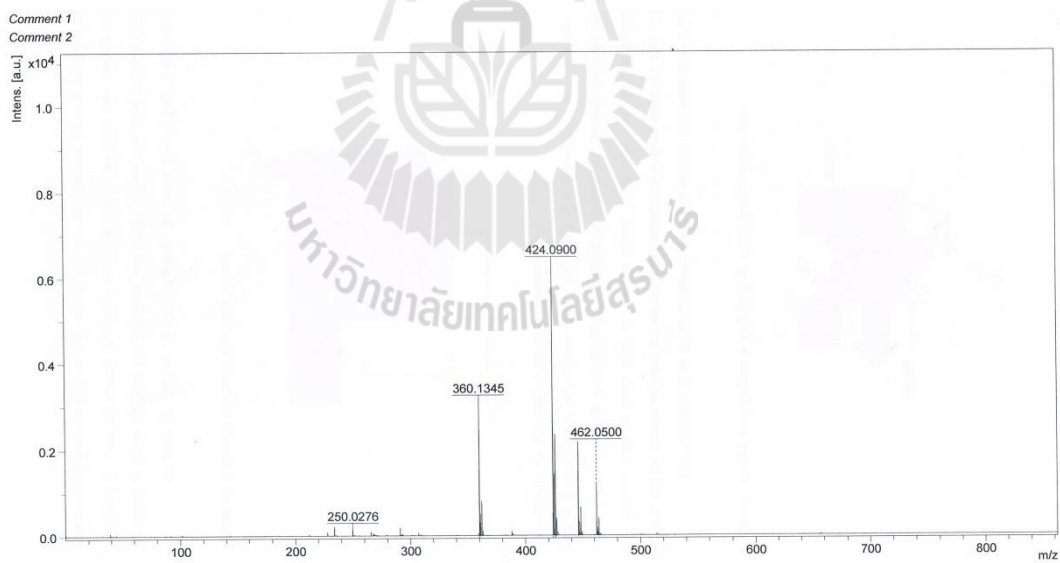
A.6.1 Mass spectrum of compound 2



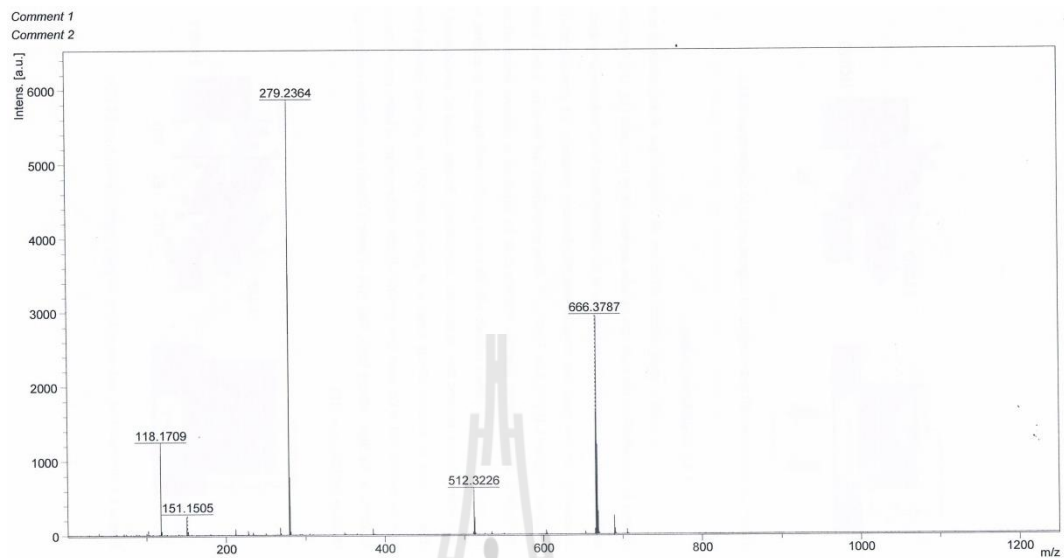
A.6.2 Mass spectrum of **compound 3**



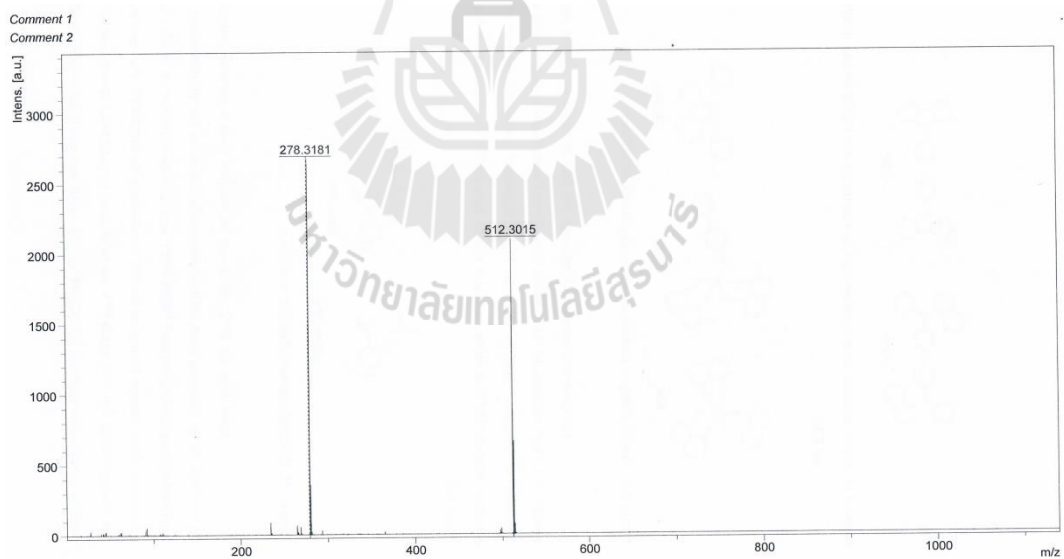
A.6.3 Mass spectrum of **compound 4**



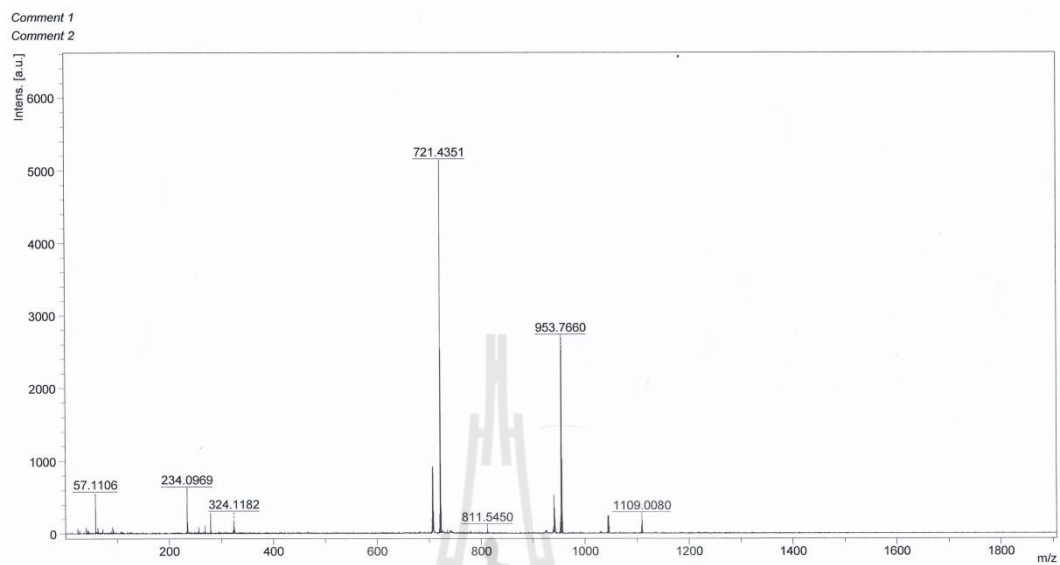
A.6.4 Mass spectrum of HQOTsG1



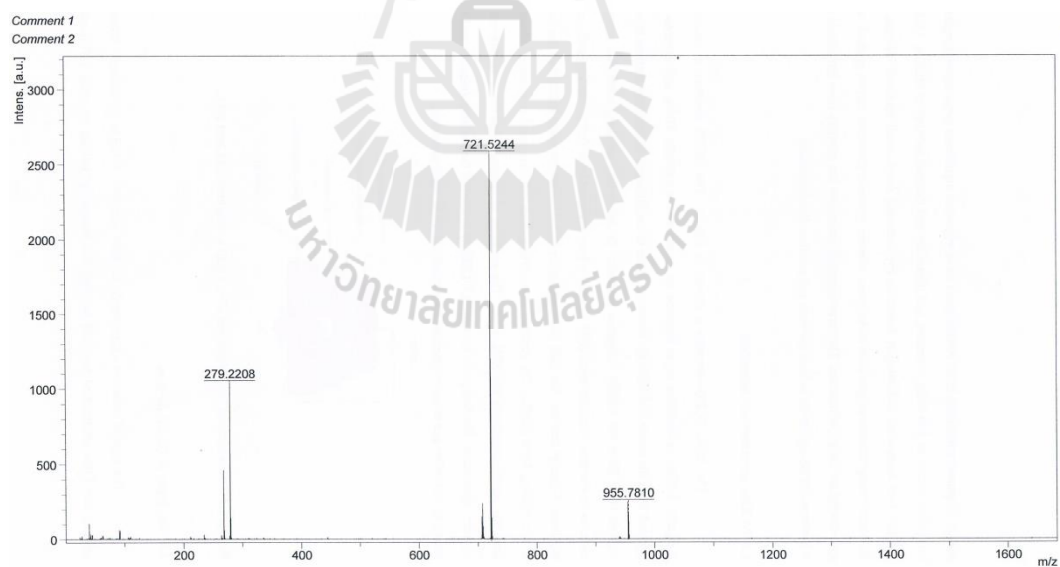
A.6.5 Mass spectrum of HQG1



A.6.6 Mass spectrum of HQOTsG2



A.6.7 Mass spectrum of HQG2



APPENDIX B

THESIS OUTPUT

Uerb-im, P., Vao-soongnern, V., and Promarak, V. (2015). “Synthesis and characterization of hole-transporting materials based on 8-hydroxyquinoline derivatives for organic light-emitting diodes (OLEDs)”, The 41st Congress on Science and Technology of Thailand (STT 41) Suranaree University of Technology, Nakhon Ratchasima 6-8 November 2015. PP 202-207 (Oral presentation)



CURRICULUM VITAE

Name Mister Panya uerb-im

Date of Birth December 7th, 1990, Buriram, Thailand

Address 98 Moo 7, Isan district, Maung District, Buriram Province, Thailand,
31000

Education

2009-2012 B.Sc. Second Class Honors (Chemistry), Khon Kaen University,
Thailand

2013-present Student at school of chemistry, Suranaree University of Technology,
Thailand with scholarship from Suranaree University of Technology

